Control of Rab Small G-Proteins in Yeast Endosomal Traffic

Andrew Logan Paulsel

A dissertation
submitted in partial fulfillment of the
requirements for the degree of

DOCTOR OF PHILOSOPHY

University of Washington

2013

Reading Committee:

Alex Merz, Chair
Peter Brzovic
Alan Weiner

Program Authorized to Offer Degree:

Department of Biochemistry

This dissertation is dedicated to my family,

whose love and support contributed greatly to this work.

Optimus magister, bonus liber.

Acknowledgements

I'd like to thank my committee members, Michael Ailion, Peter Brzovic, Rich Gardner and Alan Weiner for their frank criticisms and enumerable suggestions. All of the members of the Merz lab have helped in ways too large to count. I am most grateful to Dan Nickerson for sharing his ideas, discussion, technical assistance and time toward sections of this work. I owe many thanks to thank Rachael Plemel, Margaret Lo and Braden Lobingier for sharing multiple strains, vectors, and experimental input and discussions. Thanks as well to Chris Brett, Cortney Angers and Matt Schwartz for late night discussions and general camaraderie. Most importantly thanks to Alex Merz for sharing his passion for the endocytic system and allowing me to work in his lab. Finally, I'd like to thank my family for their support and encouragement, especially my husband who remained gallant and helpful even on my worst of days.

University of Washington

Abstract

Control of Rab Small G-Proteins in Yeast Endosomal Traffic

Andrew Logan Paulsel

Chair of the Supervisory Committee:

Professor Alexey J. Merz, Ph.D.

Department of Biochemistry

The protein trafficking pathway in eukaryotic cells is essential for maintenance of organelle identity, nutrient uptake, and adaptation to extracellular stimuli. The endocytic pathway is tasked with uptake of plasma membrane receptors and bulk extra-cellular material as well as interaction with the secretory pathway. The Rab5 family of small GTPases are essential in maintaining the endocytic pathway.

Rab5 proteins are active only when bound to GTP. Due to the slow intrinsic rate of GTP loading, Rab5 relies on the VPS9 domain for activation. VPS9 domains are highly conserved and function as activators of Rab5 by promoting GDP release and GTP loading. The diversity of members of the Rab5 subfamily and their activators indicates that this family may multiple roles in endocytosis. VPS9-domain proteins are themselves highly regulated. An emerging theory in this field suggests that modulating their localization may influence Rab5 localization and therefore function.

To address this I investigate possible regulatory roles of *Saccharomyces cerevisiae* Vps9 as influenced by ubiquitin. Yeast Vps9 can both bind ubiquitin and become ubiquitylated, though it has remained unclear what, if any, influence these functions have on Vps9 activity. These studies lead to the discovery of Muk1, an alternate yeast Rab5 activator with a VPS9-domain.

The yeast vacuole or mammalian lysosome is considered the terminal compartment of endocytosis and the HOPS protein complex is essential for regulating membrane fusion at this organelle. This complex contains several carboxy-terminal RING domains. While most RING domains have been shown to possess E3 ubiquitin ligase activity, the HOPS RING domains remain largely uncharacterized. Finally, I examined HOPS RING domain mutants to address their function for vacuole morphology and their relation to ubiquitin.

Table of Contents

Published Work

Patents

"Compositions of aminoacyl-tRNA synthetases and uses thereof."
A. Paulsel and H. Cho
U.S. Patent Application 20090123971. Filed December 2005. Published June 2006.

Publications

"Subunit organization and Rab interactions of Vps-C protein complexes that control endolysosomal membrane trafficking"
R. Plemel, B. Lobingier, C. Brett, D. Nickerson, C. Angers, **A. Paulsel**, D. Sprague & A. Merz
MBOC 2010

"Vps9 family protein Muk1 is the second Rab5 guanosine nucleotide exchange factor in budding yeast."
A. Paulsel, A. Merz, and D. Nickerson
J. Biol. Chem. 2013

List of Figures

Chapter 1

Chapter 2

Chapter 3

Chapter 4

List of Abbreviations

°	degree
D	gene deletion
3-AT	3-aminotriazole
aa	amino acid
ALP	alkaline phosphatase
BSA	bovine serum albumin
C	Celsius
CBZ-PheLeu	CBZ-phenylalanyleucine
COPI	coat protein I
CORVET	Vps-C Core Vacuole Endosomal Tethering
CPS	Carboxypeptidase S
CPY	Carboxypeptidase S
CUE	coupling of ubiquitin ER to degradation domain
DENN	Differentially Expressed in Normal and Neoplasia
DH	Dbl homology
DNA	deoxyribonucleic acid
DOGS-NTA	1,2-di-(9Z-octadecenoyl)-*sN*-glycero-3-[(N-(5-amino-1-carboxypentyl)iminodiacetic acid)succinyl
DTT	dithiothreitol
EDTA	ethylenediaminetetraacetic acid
ER	endoplasmic reticulum
ESCRT	endosomal sorting complex required for transport
fLUC	firefly luciferase
g	gram
g	force of gravity
GAP	GTPase activating protein
GARP	Golgi associated retrograde protein complex
GDI	guanosine nucleotide disassociation inhibitor

GDP	guanosine diphosphate
GEF	guanosine nucleotide exchange factor
GFP	green fluorescent protein
GGA	Golgi-localizing, γ-adaptin ear homology domain
GST	glutathione S-transferase
GTP	guanosine triphosphate
H_6	hexahistadine
HECT	homologous to E6-AP carboxyl terminus
HOPS	homotypic fusion and protein sorting complex
ILV	intraluminal vesicle
inv	invertase
IPTG	isopropyl β-d-thiogalactoside
kDa	kilodalton
L	liter
LB	Luria-Bertani
LUCID	luciferase reporter of intraluminal deposition
M	molar
mant	*N*-methylanthranioyl
MBP	maltose binding protein
MESG	2-amino-6-mercapto-7-methpurine riboside
mg	milligram
ml	milliliter
mM	millimolar
Muk	computationally linked to Kap95
MVB	multivesicular body
nm	nanomolar
PAGE	polyacrylamide gel electrophoresis
PBS	phosphate buffered saline
PBST	phosphate buffer saline with Tween-20

PCR	polymerase chain reaction
Pep	carboxypeptidase Y-deficient
PH	Plekstrin homology
PNP	purine nucleoside phosphorylase
PrA	proteinase A
RING	really interesting new gene
rLUC	Renilla luciferase
SDS	sodium dodecyl sulfate
SNARE	soluble N-ethylmaleamide-sensitive factor attachment protein receptor
TEV	tobacco etch virus
Ub	ubiquitin
UBA	Ubiquitin associated
UEV	Ubiquitin E2 variant
UIM	Ubiquitin interacting motif
VPL	vacuole protein localization
VPS	vacuole protein sorting
VPT	vacuole protein transport
Y2H	yeast-two-hybrid
YPD	yeast protein dextrose
YPT	yeast protein required for transport
µg	microgram
µM	micromolar

Overview and Literature Review

Introduction

Organelles are a quintessential feature of the eukaryotic cell. These membrane-bound compartments allow the cell to construct unique biochemical microenvironments which contain disparate or opposing biochemistries. Proper function of organelle microenvironments depends on the cell's ability to regulate incoming and outgoing proteins, lipids, and other small molecules for each compartment via transport pathways.

Cellular transport pathways can be broadly categorized into the secretory and endocytic networks, though there are multiple cross-pathway connections and specialty networks for unique cell types. The secretory pathway begins in the endoplasmic reticulum (ER) with transport through the Golgi for either cellular secretion or transport to terminal organelles. Conversely, the endocytic network is tasked with the import of extracellular material or the internalization of proteins and lipids from the cell surface and the subsequent sorting and transport of these materials (Figure 0-1).

Early and late endocytic compartments accept inbound traffic from the plasma membrane and biosynthetic traffic from the Golgi. Rab5, a small G-protein of the Ras superfamily, is found throughout these compartments and is essential to regulate membrane fusion at these organelles. Small Rab G-proteins possess low levels of intrinsic activation and rely on guanine nucleotide exchange factors (GEFs) to generate active Rab5-GTP complexes. The fact that Rab5 positive membranes serve as a convergence point for the endocytic and secretory pathways simply underscores the importance of Rab5 proteins and their GEFs for cellular homeostasis.

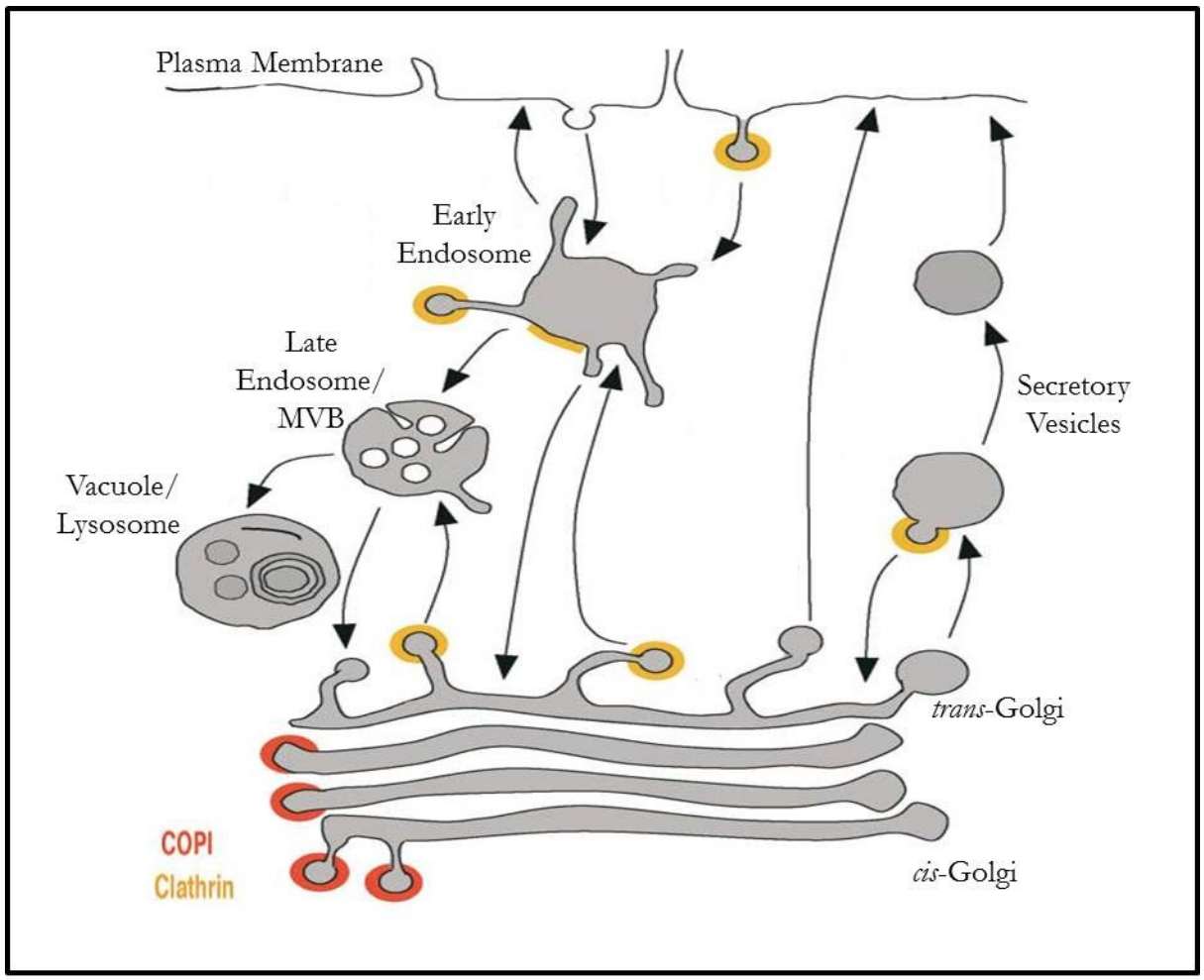

Figure 0-1 Overview of yeast endocytic and secretory pathways.

Genetics of Endolysosomal Traffic in Yeast

The yeast vacuole is an acidic organelle involved in protein and lipid degradation as well as amino acid storage, osmoregulation, and the sequestration of toxic metal ions in the cell. It is the functional equivalent of the mammalian lysosome and has been widely studied due to the ease of genetic manipulation in yeast as well as the highly conserved nature of the pathways and regulatory genes involved [1].

The secretory pathway is responsible for the delivery of resident hydrolases to the vacuole which involves synthesis at the endoplasmic reticulum followed by transit through the Golgi bodies [2]. At the *trans*-Golgi, vacuolar cargo must be packaged for delivery to the vacuole and sorted away from proteins destined for secretion. Defects at these sorting and packaging steps often result in the failure of Golgi-Vacuole transport and the mislocalization of multiple cargo proteins.

Carboxypeptidase Y (CPY; product of the *PRC1* gene) is a soluble protein which is transported through the Golgi to early endosomes en route to the vacuole lumen where it functions as a lytic enzyme. Like other soluble *trans*-Golgi cargo destined for the endocytic pathway, it contains sorting peptide motifs recognized by the receptor Vps10 [3] Cytosolic proteins interact with the cytosolic terminus of Vps10 and coordinate with Golgi small G-protein to package the Cargo-Vps10 complex into clathrin coated vesicles which then bud from the trans-Golgi [4; 5]. These vesicles target, dock, and fuse with early endosomal compartments through the activity of several Class D gene products.

Examination of CPY trafficking defects has provided a means to investigate membrane trafficking along this route. This is primarily due to the fact that genetic or chemically induced disruptions of this pathway frequently result in the accumulation of CPY at the trans-Golgi where it becomes incorrectly packaged and secreted from the cell. This secretion phenomena has been used as the basis for several genetic and biochemical screens to identify the components of the vacuolar protein targeting pathway [2; 6; 7]. Elizabeth Jones and colleagues used a colorimetric CPY substrate to identify mutant yeast cells with reduced peptidase (*pep*) activity [6]. Tom Stevens and his coworkers devised an elegant genetic selection using a modified phenylalanine-leucine dipeptide (CBZ-PheLeu) which is cleaved by CPY, freeing leucine for cellular consumption. While activation of CPY is normally dependent on the resident vacuolar hydrolase proteinase A (PrA), secreted CPY is able to free leucine from CBZ-PheLeu in its zymogen form. Leucine auxotrophs lacking PrA are only able to grow on CBZ-PheLeu when sorting is disrupted and CPY is secreted. Thus, mutagenized yeast plated on CBZ-PheLeu were used to identify vacuole protein localization mutants (*vpl*) [8]. Concurrently, Scott Emr used a CPY-invertase fusion to identify vacuolar protein targeting (*vpt*) mutants. Wild-type yeast secrete invertase (inv) into the periplasm for sucrose metabolism. However, translational fusion of inv and CPY (CPY-inv) results in invertase targeting to the vacuole, blocking sucrose metabolism. Mutagenized yeast harboring CPY-inv were then selected for growth on sucrose plates, which identified CPY-inv missorting and secretion from the trans-Golgi [7]. Cloning and sequencing of the *PEP*, *VPL*, and *VPT* genes resulted in the identification of a panoply of genes (currently >70), many of which were identified in multiple screens. To simplify matters the genes were categorized into vacuole protein sorting (*vps*) complementation groups and classified (Class A-F) based on vacuole morphology when deleted [9].

Vacuole morphology can be determined using vital dyes such as CDCFDA and lipophilic styryl dyes, which are internalized and trafficked through the endocytic pathway and ultimately reach the vacuolar limiting membrane. Wild-type cells generally contain one to three spherical vacuoles, while genetic defects in endocytic trafficking genes result in various aberrant vacuolar morphologies which have been categorized into six classes. Class A (*e.g., vps10, vps13, vps29, vps30, vps35, and vps38*) vacuole mutants exhibit wild-type vacuolar morphology. Class B mutants (*e.g., vps5, vps17, vps39,*

vps41, and vps43) show a fragmented vacuolar phenotype, with a large number of smaller vacuoles filling the cell (usually >5). These mutants include proteins required for vacuolar homotypic fusion (*vps39, vps41*) as well as subunits of the retromer complex (*vps5*, *vps17*), which is involved in retrograde trafficking from the endosome to the Golgi. Class C mutants (*e.g., vps11, vps16, vps18, and vps33*) have strong sorting and conditional growth defects and contain no vacuole, but rather display a haze of small endocytic puncta which are distributed throughout the cell. The four Class C mutants were later shown to form a tetrameric protein complex (Vps-C Core) which is an essential part of the HOPS (**HO**motypic fusion and **P**rotein **S**orting) complex at the vacuole and CORVET (Vps-**C** c**OR**e **V**acuole **E**ndosomal **T**ethering) complex at the late endosome/multivesicular body (MVB). Class D mutants (*e.g., vps3, vps6, vps9, vps15, vps21, vps34, and vps45*) contain a single enlarged vacuole and appear to affect transport of vesicles from Golgi to endosomes or retrograde traffic from the vacuole to the Golgi. Notable Class D mutants including the yeast Rab5 ortholog Vps21 and its guanine nucleotide exchange factor Vps9 will be discussed in detail in subsequent chapters. Vacuoles in class E mutants (*vps2, vps4, vps20, vps22, vps23, vps24, vps25, vps27, vps28, vps31, vps36, vps37, and vps44*) appear normal. However, a large perivacuolar compartment is formed in Class E mutants and these cells fail to form late endosomes/multivesicular bodies (MVBs). Class E proteins include subunits of the ESCRT (**E**ndosomal **S**orting **C**omplex **R**equired for **T**ransport) complexes which control MVB biogenesis [10-13]. Class F mutants (*vps1*, *vps26*) exhibit intermediate phenotypes between wild type vacuoles and the enlarged vacuole phenotypes found in Class B mutants.

Trans-Golgi to Endosome Transport

There are multiple stages of CPY transit which, when disrupted, result in CPY secretion. One example is disruption of Class D genes which regulate fusion of *trans*-Golgi derived vesicles with early endosomes. Vps21 (Class D) is the predominant endocytic Rab G-protein and like other Rab proteins serves to coordinate and regulate membrane fusion at its resident membranes. It functions at multiple membranes in the endocytic pathway and is the primary yeast homology of mammalian Rab5. Like all Rab G-proteins, Vps21 becomes active upon binding the nucleotide GTP and inactive when GDP bound. Due to the slow intrinsic rates of GTP hydrolysis and GDP release, Vps21 relies on regulatory proteins to facilitate the G-protein cycle. Vps9 is the GEF (**G**uanine nucleotide **E**xchange **F**actor) which promotes disassociation of GDP, allowing the more-abundant GTP to enter and activate Vps21 [14; 15]. Conversely, GAPs (**G-protein** **A**ccelerating **P**roteins) interact with GTP-Vps21, stimulating GTP hydrolysis and deactivating the Rab [16]. Several models have been proposed for GEF and GAP recruitment and regulation, though to date it is unclear if there is a unifying regulatory mechanism for these proteins.

Once active, GTP-Vps21 interacts with the effector protein Vac1 (Vps19) which in turn recruits Vps45, a Sec1 family SNARE cofactor [17; 18]. Vps45, like all Sec1 family proteins, facilitates SNARE activity, which in turn drive membrane fusion by association with endocytic SNAREs including Pep12 (Vps6) and Vti1 [19; 20]. Concurrently, a kinase complex comprised of Vps15 and Vps34 (both Class D) generates phosphatidylinositol-3-phosphate (PI(3)P) at early endosomal membranes, which recruits Vac1 to this surface via two tandem FYVE domains [17; 18]. Thus, Vac1 is recruited to endosomes though generation of Vps21-GTP via Vps9 activation and generation of PI(3)P, allowing for recruitment of Vps45 and coordination of SNARE activity to catalyze membrane fusion [21]. As shown by our lab, Ungermann's, and others, Vps21 also recruits a second effector complex (CORVET) that contains Vps33, another Sec1 family member which is a component of the Vps-C core (see below and Chapter 4).

Once trans-Golgi derived vesicles fuse with early endocytic compartments, Vps10 is recycled back to the Golgi for further rounds of transport. Class A genes Vps29 and Vps35 form a complex which interacts with the cytosolic tail of Vps10 at the endosome [22]. This complex along with the sorting nexins Vps5 and Vps17 along with Vps26 form the pentameric retromer complex at the early endosome, which interacts with PI(3)P at the endosome via a PX domain [23; 24].While it is unclear if the retromer proteins act as a true protein coat akin to clathrin, they have been shown to drive clathrin-independent membrane tubulation at the endosome [25]. Ypt6, the Rab G-protein at the Golgi, regulates the incoming retrograde membrane and coordinates with the **G**olgi-**a**ssociated **r**etrograde **p**rotein complex (GARP: Vps51, Vps52, Vps52, Vps54). GARP interacts with SNAREs and Ypt6 to regulate vesicle fusion at the Golgi [26-28].

Early Endosomal Trafficking

As early endosomes accept cargo from the secretory trans-Golgi network, they must also facilitate incoming vesicles from the plasma membrane via endocytosis. The internalization of transmembrane transporters and receptors from the plasma membrane is a key regulatory feature in the cell. Mono-ubiquitylation of proteins at the plasma membrane is a common signal for their internalization [29; 30]. Transporters such as the amino acid permeases Mup1 and Gap1, and the uracil permease Fur4 become ubiquitylated as a result of environmental cues which target them for internalization. Similarly, the mating factor receptor Ste3 is constitutively ubiquitylated and internalized. This serves to dampen the signaling cascade when mating factor is absent [31-33]. These plasma membrane proteins, along with many others, are ubiquitylated by Rsp5, a HECT-E3 ubiquitin ligase orthologous to mammalian Nedd4 [34]. Once tagged with a ubiquityl moiety, ubiquitin interaction motifs (UIMs) found in epsins Ent1 and Ent2 help to sort and coordinate the endocytic internalization of these cargo-ubiquitin molecules via interactions with the AP2 complex and clathrin [35].

Ubiquitin is a 76 amino acid protein and is widely conserved in eukaryotic cells. It becomes covalently attached to surface lysines on protein substrates via its carboxy-terminus in a tri-enzymatic cascade reaction. First, free ubiquitin is attached to an ubiquitin activating enzyme (E1) in an ATP dependent manner. This E1 then transfers ubiquitin to an ubiquitin conjugating enzyme (E2) which, in turn, transfers ubiquitin to the substrate with the help of an ubiquitin protein ligase (E3) [36]. Two types of E3 ligases have been found: RING motif E3 ligases coordinate direct transfer of ubiquitin to the substrate while HECT-E3 ligases transfer the ubiquitin to themselves before passing it onto the substrate [34; 37]. This reaction can then stop by forming a mono-ubiquitylated cargo or continue, either transferring ubiquitin to multiple lysines on the substrate (multi-mono-ubiquitylation) or by creating poly-ubiquitin chains by transferring incoming ubiquitin to surface lysine residues on previous ubiquityl moieties. Since ubiquitin itself has multiple lysines, the cell uses different linkages of poly-ubiquitin for a variety of signals. However, endocytic events appear to be marked predominantly by single or multiple mono-ubiquitin transfer events (mono- or multi-ubiquitylation vs. poly-ubiquitylation) [29].

Several domains have been identified which bind ubiquitin with a wide range of affinities. The ubiquitin interaction motif (UIM), the ubiquitin-associated domain (UBA) and the coupling of ubiquitin-conjugation to ER degradation (CUE) domain all interact with ubiquitin with a wide range of affinities (15-400 uM)[38-41]. The CUE domain found in Vps9 will be discussed in detail in later chapters.

Late Endosomal/Multivesicular Body Trafficking

Unlike the trafficking of soluble CPY via the receptor Vps10, carboxypeptidase S (CPS) is a transmembrane protein which requires additional steps for delivery to the vacuole. Initially trafficked much like Vps10 from the trans-Golgi, CPS is retained on the early endosomal membrane where it becomes mono-ubiquitylated, similar to internalized cargo from the plasma membrane [42]. While it is unclear what marks the transition from early to late endosomes, one prevailing model points to the presence of mono-ubiquitylated cargo on the endosomal membrane. As CPS-Ub and other ubiquitin tagged cargos are internalized from the plasma membrane or sorted from the *trans*-Golgi, subunits of various ESCRT complexes recognize the ubiquitin modifications via several ubiquitin binding domains. The four ESCRT complexes (ESCRT-0, ESCRT-I, ESCRT-II, and ESCRT-III) contain multiple ubiquitin binding domains and sequentially recognize the ubiquitylated cargo on the endocytic membranes via these domains. The complexes then act to sequester the cargo, packaging it into budding intraluminal vesicles while removing ubiquitin and finally releasing the budding vesicles into the endosomal lumen.

One initial recognition event of ESCRT-0 relies on VHS and UIM ubiquitin binding domains of Vps27 and Hse1 as well as an interaction between the FYVE domain in Vps27 and PI(3)P on the endosomal surface [43; 44]. ESCRT-I (Vps23, Vps28, and Vps37) is then recruited via an ubiquitin binding domain in Vps23 (UEV domain) [42], which then recruits ESCRT-II (Vps22, Vps25, and Vps36) [11]. The ESCRT-III complex (Vps20, Vps32, Vps2, and Vps24) associates with the previous ESCRT complexes further sequestering the cargo and deforming the membrane. The complex is ultimately disassembled by Vps4, a AAA-ATPase which is essential for the ESCRT complex release and recycling [10; 45; 46]. In the final stages of ESCRT recruitment and vesicle budding, the ubiquitin moieties are removed by the deubiquitylase Doa4 and the internal buds scission, creating small cargo loaded intraluminal vesicles within the endosomal lumen. As this process continues the lumen becomes filled with intraluminal vesicles and creates the identifiable MVB.

Defects in the MVB sorting process can retain cargo on the endosomal limiting membrane which, upon fusion with the vacuole, results in their localization to the vacuolar limiting membrane rather than their degradation in the vacuole lumen. This can clearly be seen with CPS trafficking defects. The CORVET protein complex is responsible for coordinating membrane fusion at this organelle. Comprised of the Vps-C Core and two accessory proteins (Vps8, Vps3), CORVET interacts with active Vps21-GTP to coordinate vesicle tethering, docking, and membrane fusion.

As endosomes mature into MVB they ultimately undergo fusion with the vacuole. This process involves a Rab transition from endocytic Vps21 (Rab5) to vacuolar Ypt7 (Rab7) [47]. Concurrently, the CORVET complex is replaced by HOPS which interacts with active Ypt7-GTP to coordinate fusion at this membrane [48]. HOPS contains the same Vps-C core (Vps11, Vps16, Vps18, and Vps33) as CORVET, but interacts with two different accessory proteins (Vps39, Vps41). It remains unclear if the transition from MVB to vacuoles results in the remodeling of CORVET to HOPS or if the two complex are static at their respective membranes [49]. The protein components of the Vps-C core are essential for the integrity of this pathway, while deletions or mutations in the four accessory proteins display less overt phenotypes (Vps3, Vps8 – Class D, Vps39, Vps41—Class B).

Research Aims

Rab5 G-protein family members in the endocytic pathway are highly conserved and function to coordinate and regulate vesicle fusion at this complex organelle. The VPS9-domain is highly conserved in eukaryotic cells and appears to be the sole catalytic domain for nucleotide exchange and activation of the Rab5 subfamily. As such, it is essential for proper endocytic function. I am interested in how the VPS9-domain localizes to Rab5 positive membranes as well as how it is itself regulated.

Due to the highly conserved nature of these genes in eukaryotes, yeast has provided an excellent model organism for dissecting these pathways. While several models of Vps9 localization have been proposed, they have remained difficult to test for several reasons. The yeast Rab5 GEF, Vps9, has two ubiquitin related functions: ubiquitin binding and covalent modification with ubiquitin. Each of these appears to be important in Vps9 regulation; however, both features rely on the CUE domain, a C-terminal high affinity ubiquitin binding domain. Mutations in this domain affect both ubiquitin binding and Vps9 ubiquitylation and make it difficult to determine how these two facets affect Vps9 regulation.

My examination of *in vivo* CUE domain mutants resulted in little to no phenotypes (Chapter 2). This was surprising since previous data indicate the CUE domain to be critical for Vps9 function. These experiments lead to the investigation of alternative Rab5 GEFs which may not have appeared in the initial set of vps screens. I identified Muk1 as an alternative Rab5 GEF and hypothesize that its presence may have masked any phenotypes associated with Vps9 CUE domain mutation or deletion (Chapter 3).

I also worked on a collaborative project in the Merz lab examining the organizational structure of the HOPS and CORVET protein complex. As mentioned above, the Vps-C Core is an obligate feature of the vacuolar HOPS and endosomal CORVET complexes which made dissecting and examining the architecture of these complexes difficult. Using a combination of yeast-two-hybrid, *in vitro* biochemistry, and vacuole morphology phenotypes we mapped and examined several interaction domains of the Vps-C core with its accessory proteins. Half of these proteins contain C-terminal RING-like motifs (Vps8, Vps11, Vps18, Vps39). Three of the four RING-like domains are conserved from yeast to humans, with the fourth RING domain in yeast (scVps39) conserved in the neighboring accessory protein in the same HOPS holocomplex in humans (hsVps41). The roles of these domains in complex formation and Vps-C complex function are explored in Chapter 4.

Characterization of Vps9 and the CUE Domain

Introduction

Small Rab G-proteins are the largest subset of the Ras G-protein superfamily and are key regulators of membrane fusion events in eukaryotic cells. Rabs are highly conserved, with at least 11 Rabs identified in yeast and more than 60 in humans [50]. Rab5 and Rab7 are the two key Rabs in the endocytic pathway occurring at the endosomal and vacuolar membranes, respectively. Both are essential in the targeting and fusion of vesicles to their resident membranes as well as the homotypic fusion of these organelles [51; 52]. Rab5 has also been shown to stimulate vesicle motility along microtubules, an example of ancillary roles for Rabs outside of classical membrane fusion [53].

Mammals possess three Rab5 isoforms (Rab5a, Rab5b, and Rab5c) and each has been shown to possess unique activity *in vivo* [54]. Similarly, yeast contain three Rab5 isoforms (Vps21/Ypt51, Ypt52, and Ypt53) which have also been shown to coordinate specific events in the cell [55]. Both the yeast and human Rab5 subfamilies show a high degree of sequence homology similarity. The fact that mammalian Rab5 can be activated by yeast GEFs underscores this similarity [18]. Vps21 appears to be the predominant Rab5 paralog in yeast, though studies suggest Ypt52 and Ypt53 are partially redundant [55]. Like mammalian Rab5, Vps21 is necessary for delivery of cargo from the Golgi and plasma membranes to endosomes [56].

As briefly described in Chapter 1, Rabs are regulated through the binding of guanine nucleotides, becoming active when GTP bound and inactive when bound to GDP. Due to the low intrinsic rate of GTP hydrolysis and GDP release, Rab G-proteins require accessory proteins to modulate their active state. Guanine nucleotide exchange factors possess higher affinities toward Rab-GDP and catalyze the opening of the nucleotide binding pocket, allowing GDP release and freeing the pocket for GTP to enter. Due to the lower affinity toward Rab-GTP GEFs are displaced once GTP is bound, allowing the active Rab to interact with downstream effector molecules to coordinate membrane fusion events. GEFs are highly specific toward Rabs or Rab subfamilies and appear to possess highly conserved catalytic domains. For example, GEFs toward Arf, Ras, and Rho G-proteins have been shown to contain Sec7, Cdc25, and DH/PH (Dbl Homology/Plecktrin homology) domains, respectively [57]. Likewise, a large family of Rab GEFs contain a DENN (**D**ifferentially **E**xpressed in **N**ormal and **N**eoplasia) domain, though not all do [58]. G-protein accelerating proteins (GAPs) fulfill the remaining half of the Rab cycle by catalyzing GTP hydrolysis to deactivate Rabs. Unlike GEFs, Rab GAPs appear to possess a broader specificity toward Rab families.

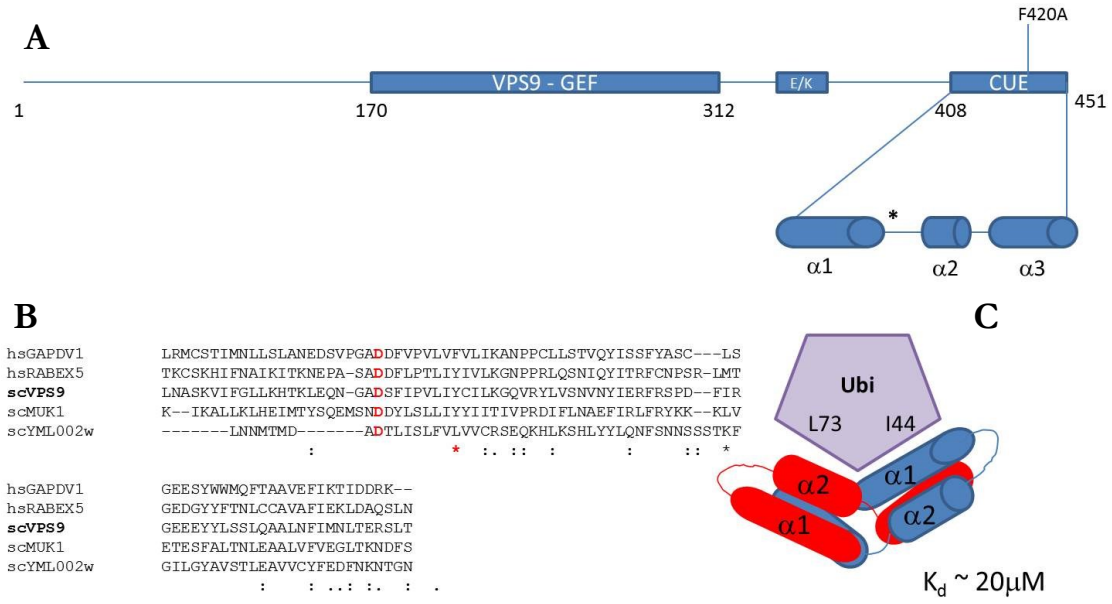

Figure 0-1 (A) Domain architecture of yeast Vps9. (B) VPS9-Domain alignment for two human proteins and three yeast proteins. (C) Cartoon of yeast Vps9 CUE domain interaction with ubiquitin.

The VPS9-domain has been shown as the catalytic GEF domain toward the Rab5 subfamily in both yeast and humans [14; 59; 60]. This domain is widely conserved in eukaryotes with two VPS9-domains in *S. cerevisiae* (scVps9, scMuk1), three in *C. elegans* (RME-6, RABX-5, and CE23604), four in in *D. melanogaster* (Sprint, CG9139-PA, CG1657-PA, and CG7158-PA) and at least nine in humans (Figure 0-1b). The VPS9-domain has been shown to catalyze Rab5-GDP disassociation in at least nine of these VPS9-domain positive proteins, indicating that this is the conserved Rab5 GEF in eukaryotic cells [15; 59-62].

Kinetic studies of the VPS9-domain, both the yeast Vps9 and mammalian Rab5, indicate that the VPS9-domain possess a lower catalytic exchange rate towards Rab5 than other GEF domains [63]. While the reasons for this lower activity are unclear, it is interesting that the catalytic VPS9-domains from both yeast and humans are stronger when the remainder of the protein is absent, possibly indicating that proteins in the Vps9 family undergo some type of intermolecular regulation. One proposed regulatory method is the high affinity interaction between the c-terminal Vps9 CUE domain and a covalently attached ubiquityl moiety on Vps9.

Rabex-5, the primary mammalian Rab5 GEF, and Vps9 have been well characterized and striking similarities found. Not only is the central catalytic VPS9-domain highly conserved, but it appears that other regulatory features of the proteins have also been retained. As mentioned in Chapter 1, Vps9 possess a C-terminal CUE domain which dimerizes with an extremely high affinity towards ubiquitin (~20 uM) [38]. Rabex-5 possess an N-terminal A20-zinc finger which binds ubiquitin with comparable affinity (~12-22 uM) [64; 65]. The fact that the ubiquitin binding

properties of this conserved GEF remain, albeit in evolutionarily distinct domains, underscore the importance of ubiquitin binding.

The CUE domain of Vps9 binds ubiquitin with higher affinity than most ubiquitin binding domains, including other CUE domains (e.g. Cue2 domain ~155 uM) [66-68]. Structural studies of the CUE domains from Vps9 and CUE2 show that the trihelical Vps9 CUE domain is able to open while dimerized, exposing a secondary ubiquitin binding pocket [68]. This secondary pocket allows the Vps9 CUE dimer to interact with two faces of ubiquitin, effectively sandwiching it between the two CUE domains and leading to the heightened affinity (Figure 0-1). In contrast, the CUE domain from Cue2 appears to interact with a single face of ubiquitin as a monomer [66].

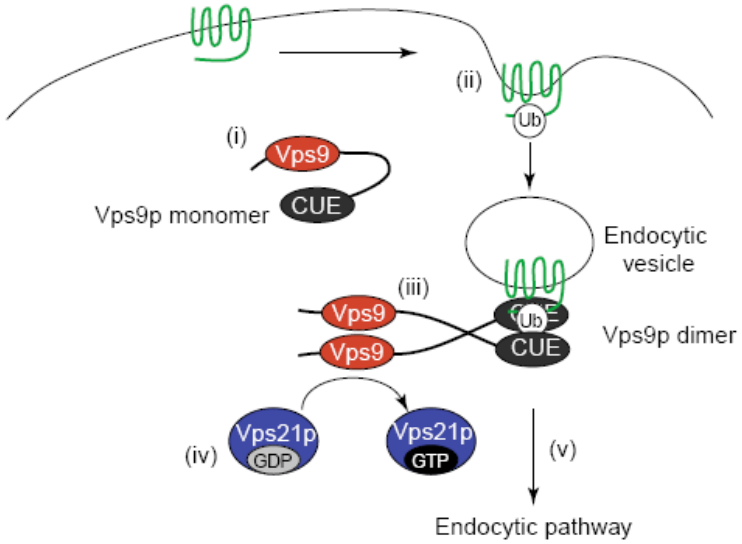

Figure 0-2 Ubiquitin binding potentiates Vps9p endocytic function in yeast.

It has been shown for some time that ubiquitin plays a key role in endocytic signaling, serving to mark receptors at the plasma membrane for internalization as well as for recruitment of ESCRT machinery at the MVB [69; 70]. The discovery that Vps9 could bind ubiquitin indicated that ubiquitin tagged cargo in the endocytic surface might be playing a broader role in protein recruitment. Studies of Vps9 lacking the CUE domain have shown that it plays a positive role in Vps9 activity at this membrane [71; 72]. Mutations in the CUE domain which abolish Vps9 dimerization, but retain monomeric ubiquitin binding, support this theory in so far as they appear to result in less efficient transport of cargo through the endocytic pathway [67]. These studies have led to a prevailing model where the CUE domain is responsible for Vps9 localization to ubiquitin positive endosomes, allowing for Vps21 activation and subsequent membrane fusion. (Figure 0-2)[73]

Interestingly, Vps9 has also been shown to be covalently modified with ubiquitin. Roughly ten percent of Vps9 appears to be ubiquitylated *in vivo* with mono-ubiquitylation being the predominant form [68; 71]. The CUE domain is essential for the ubiquitylation of Vps9 and all known mutations which abolish ubiquitin binding also reduce or eliminate Vps9 ubiquitylation. This has made the functions of CUE-dependent ubiquitin binding and the CUE-dependent ubiquitylation of Vps9 difficult to separate.

The role of Vps9 ubiquitylation is still unknown. One hypothesis is that the ubiquitylation may directly alter Vps9 catalytic activity as a method of regulating Vps21 activity. Another hypothesis is that Vps9 ubiquitylation could instead sequester the CUE domain, thus interfering with Vps9 localization to ubiquitylated cargo on endosomes and negatively affecting its ability to activate Vps21. These hypotheses are not, of course, mutually exclusive. In the studies described in this chapter I developed methods and reagents needed to test these hypotheses. I demonstrate the preparation of chemically pure mono-ubiquitylated Vps9 and demonstrate that mono-ubiquitylation of Vps9 does not interfere with its intrinsic catalytic capacity in solution-based assays.

Results

Vps9 Localization via Microscopy

The C-terminal CUE domain is currently believed to be the primary factor necessary to localize Vps9 to ubiquitin decorated endosomes where it can activate Vps21. If this model is correct, Vps9 CUE domain mutants which cannot bind ubiquitin (Vps9 F420A) should become mainly cytosolic whereas wild type Vps9 would appear on endosomal puncta. Alleles of Vps9 with N-terminal mCherry fluorescent epitopes were expressed episomally in *vps9*Δ cells in order to examine this theory. As seen in C, D both wild type and the F420A ubiquitin binding mutant appear largely cytosolic with no obvious subcellular localization. Endosomal and vacuole morphology was also examined with the intrinsic lipophilic dye FM4-64. The vacuole appears normal with both Vps9 wild type and the F420A mutant, showing that Vps9 unable to interact with ubiquitin does not drastically alter vacuolar morphology (Figure 0-3 A,B).

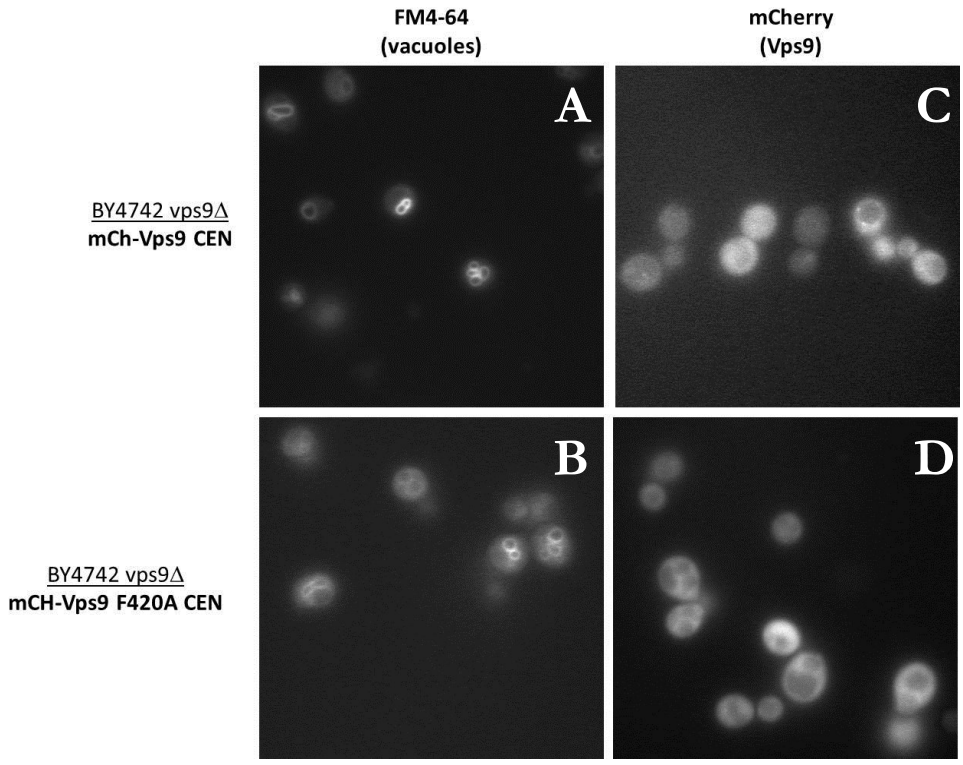

Figure 0-3 Ubiquitin null Vps9 mutation does not alter localization. Vacuoles stained with FM4-64 in cells expressing mCherry-Vps9 WT (A) or mCherry-Vps9 F420A (B). Vps9 localization with mCherry-Vps9 WT (C) or mCherry-Vps9 F420A (D).

Vps9 Localization via Differential Centrifugation

Since the emission wavelengths of mCherry and FM4-64 overlap, it was problematic to concurrently visually mCherry-Vps9 and the endosomal network. Instead, I examined mCherry-Vps9 (WT and F420A) by differential centrifugation. Briefly, log phase yeast were spheroplasted and centrifuged at a low 13,000 x g centrifugal force which pellets vacuoles, endosomes, and other large organelles, such as the nucleus and mitochondria (P13). The supernatant was decanted and subjected to a higher 100,000 x g centrifugal force to pellet small transport vesicles and Golgi bodies (P100). Finally the 100,000 x g supernatant was decanted (S100; cytosol). Each fraction was then separated by SDS-PAGE, transferred to nitrocellulose, and immunoblotted for various endocytic cargos and proteins of interest.

Blots probed with anti-RFP antibody showed mCh-Vps9 WT and F420A largely in the cytosolic S100 fraction, agreeing with previous microscopy images. The small amount of Vps9 in the P13 and P100 fractions was not altered by the F420A mutation (Figure 0-3). CPY and alkaline phosphatase (ALP) were also examined. As mentioned in Chapter 1, CPY transits through the endosomal network before maturation in the vacuole lumen. Conversely, ALP is trafficked directly from the Golgi to the vacuole where it also undergoes proteolytic maturation. Both the ALP and CPY pathway appear normal with no changes in their localization or proteolytic cleavage (Figure 0-4). This indicates that the F420A

mutant largely results a normal and functional endocytic network. Also, Vps21 localization to endosomes did not appear to be altered, nor did the obligate HOPS/CORVET subunit Vps33 (Figure 0-4).

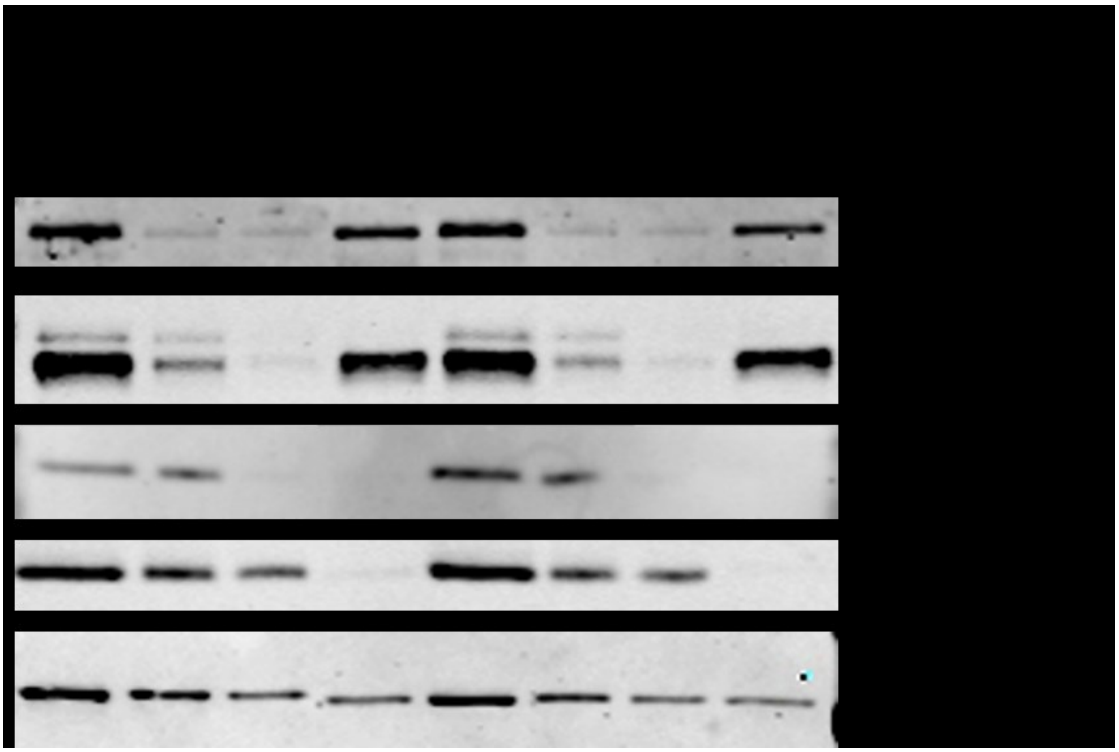

Figure 0-4 Vps9 F420A mutant is mainly cytosolic and does not appear to alter CPY or ALP trafficking or processing. Differential centrifugation of yeast expressing WT Vps9 or F420A mutant. CUE domain F420A mutant does not alter subcellular localization. CPY and ALP pathways are normal. Endosomal Vps21 and vacuolar HOPS (Vps33) also localize as WT. Vps21 and the HOPS SM protein Vps33 also appear to be localized normally.

Preparation and Purification of Mono-ubiquitylated Vps9

Due to the lack of phenotypes for the F420A mutant *in vivo*, I turned to *in vitro* biochemistry to assess the role the ubiquitylation of Vps9 may have on its catalytic activity. In order to examine the effect of mono-ubiquitylation of Vps9 I needed to develop tools to ubiquitylate and purify Vps9 .

I developed a procedure (Figure 0-5A) to express and purify mono-ubiquitylated Vps9. Briefly, Vps9 was expressed in E. coli with a N-terminal hexahistadine-maltose binding (H_6MBP) protein tag separated with a tobacco etch virus (TEV) protease linker (H_6MBP-TEV-Vps9). H_6MBP-Vps9 was purified from cell lysates on Ni-NTA resin and eluted with imidazole (Figure 0-5A, Step 1). This material was dialyzed to remove excess imidazole and subjected to *in vitro* ubiquitylation in a reaction with E1, E2, E3, and His_6-ubiquitin (Figure 0-5A, Step 2). The ubiquitylation machinery and excess ubiquitin were removed via affinity chromatography on amylose resin (Figure 0-5A, Step 3). Elution with

maltose resulted in a heterogeneous population of His_6-ubiquitylated and non-ubiquitylated H_6MBP-Vps9. This material was incubated with TEV protease (Figure 0-5A, Step 4). Cleavage products were further affinity purified over Ni-NTA resin, separating retained H_6MBP tag as well as H_6-Ub-Vps9 from non-ubiquitylated Vps9 in the flow-through (Figure 0-5A, Step 5). Mono-ubiquitylated Vps9 was then polished using size exclusion chromatography to remove the H_6MBP contaminant (Figure 0-5A, Step 6). The separation of ubiquitylated Vps9 from unmodified protein (Step 5) and the following separation from the maltose binding protein tag (Step 6) are shown in Figure 0-5B, C. Similar treatment of H_6MBP-Vps9 F420A resulted in little to no ubiquitylation as expected, as previous experiments have indicated the F420A mutant is unable to be ubiquitylated[68].

The resultant Vps9-Ub appeared mainly as mono-ubiquitylated product, with few di- and poly-ubiquitin bands which were largely removed via SEC (Figure 0-5B,C). In order to ensure this ubiquitylation reaction was reversible, the material was treated with the catalytic core of a murine ubiquitin specific protease (Usp2cc). Treatment with Usp2cc resulted in the cleavage of free ubiquitin from Vps9, showing that the ubiquitylation reaction is reversible and functioning as expected (Figure 0-5D). The final product, Vps9-Ub, is ~85% pure by SDS-PAGE.

Catalytic Activity of Vps9-Ub

I next compared Vps9 with that of Vps9-Ub. Vps9 catalyzes the release of GDP from the inactive Vps21-GDP complex, freeing the active site and allowing cytosolic GTP to enter and activate the Rab. To measure this reaction *in vitro*, I used two different assays. N'-methylanthraniloyl-GDP (mant-GDP) is a fluorescent GDP analog. The 'mant' epitope on the 3' ribose-hydroxyl of GDP is able to accept photons from excited tyrosine residues while in the nucleotide binding pocket of Vps21. This FRET pairing allows for the quantification of Vps21-mant-GDP release as a function of Vps9 catalysis.

Assay showing catalyzed Vps21-mantGDP expulsion by varying concentrations of Vps9, performed by Braden Lobingier. (Figure 0-6A). Mono-ubiquitylated Vps9 was incubated with and without deubiquitylase (Usp2cc) and used to catalyze mant-GDP release and non-ubiquitylated Vps9 from B. Lobingier was used as a control. As seen in Figure 0-6B, mono-ubiquitylated Vps9 catalyzes the release of mant-GDP with similar kinetics to de-ubiquitylated Vps9, indicating that ubiquitylation does not alter the intrinsic catalytic activity of Vps9.

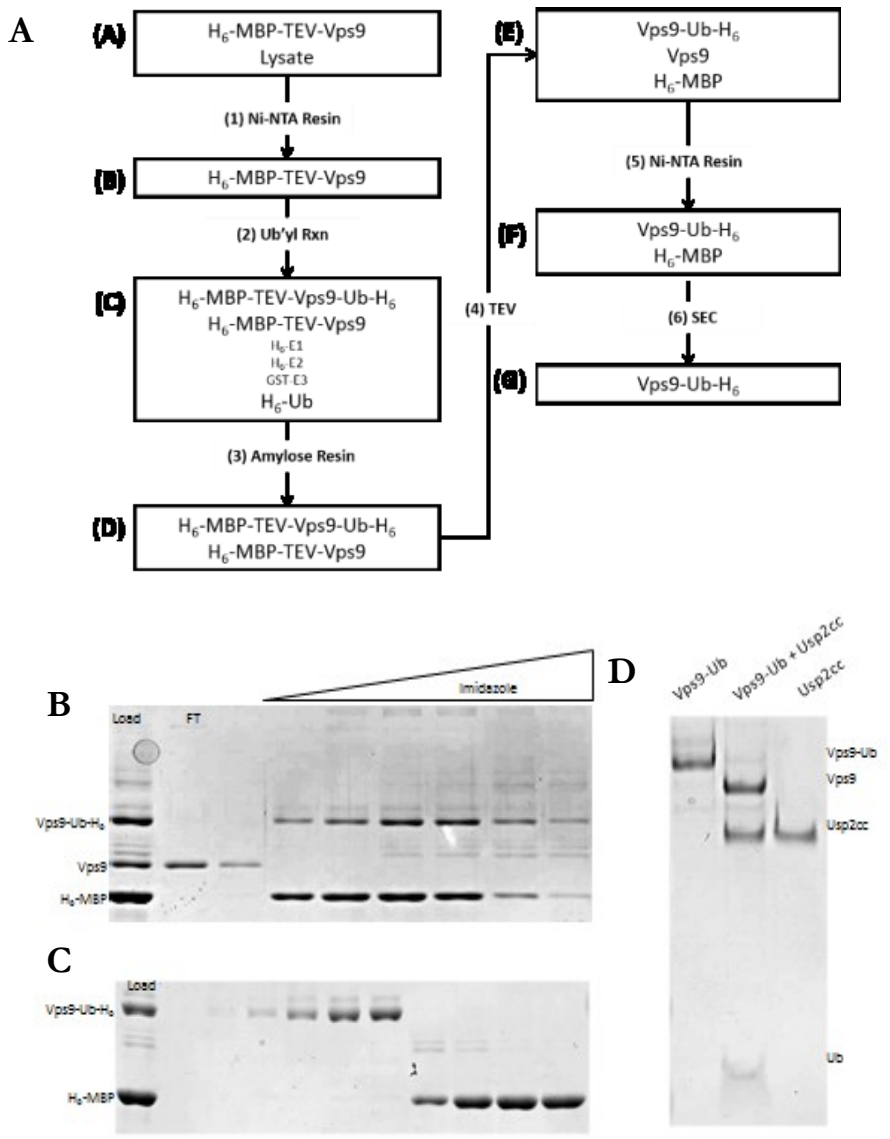

Figure 0-5 (A) Schema for the ubiquitylation and purification of Vps9-Ub. (B) Separation of Vps9 and ubiquityl-Vps9 (Step 5) (C) Final separation of ubiquitylated Vps9 from contaminating epitope tag by size exclusion chromatography (Step 6). (D) Ubiquitylation of Vps9 is reversible when treated with ubiquitin specific protease.

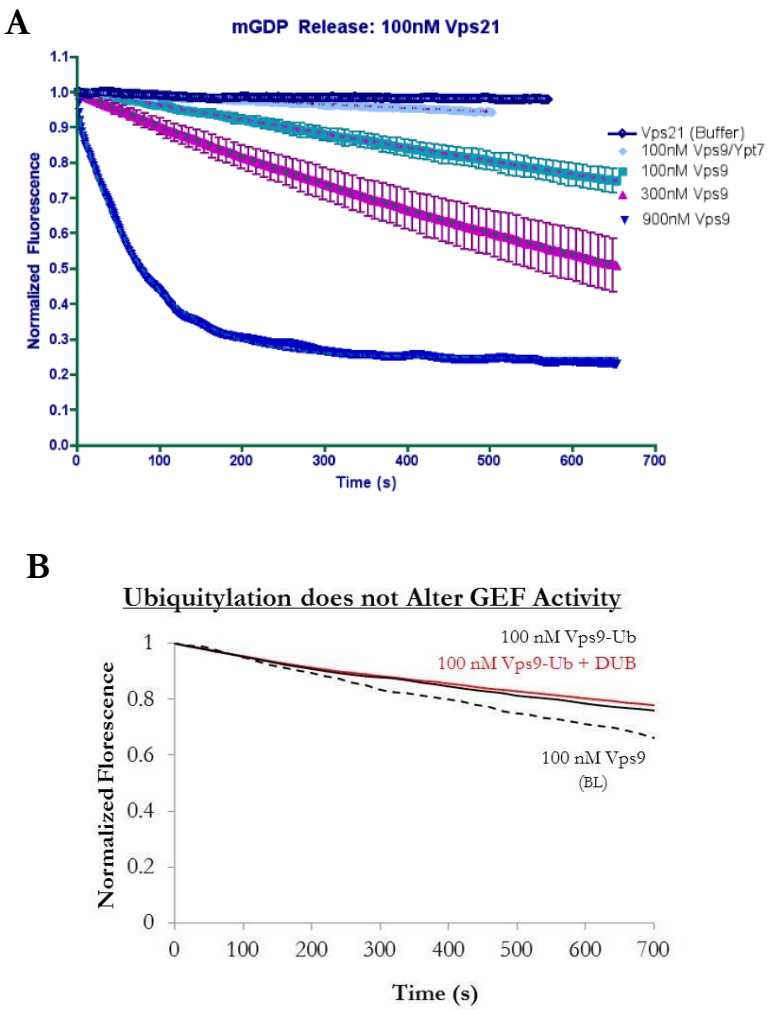

Figure 0-6(A) Vps9 acts as a Vps21 GEF. Performed by B. Lobingier (B) Ubiquitylation of Vps9 does not alter catalytic activity. Vps9-Ub was incubated with or without Usp2cc and used to catalyze mant-GDP release from Vps21. Non-ubiquitylated Vps9 from B. Lobingier was used as a control for assay-to-assay variation (dash line).

Catalytic Activity of Vps9 with Free Ubiquitin

An additional study was performed to examine the roll of free ubiquitin in Vps21 activation. In contrast to the mant-GDP expulsion assay, this assay utilized normal GDP and GTP nucleotides and instead measured the release of inorganic phosphate in order to measure Rab cycle turnover. As described above, the catalytic Rab cycle involves loading the Rab with GTP via a GEF followed by the induced hydrolysis of GTP to GDP via a GAP. As this cycle perpetuates inorganic phosphate is released and can be measured via conjugation to 2-amino-6-mercapto-7-methpurine riboside (MESG), a small molecular reporter which changes its absorbance when phosphorylated with inorganic phosphate via purine nucleoside phosphorylase (PNP). This phosphate release assay therefore measures multiple rounds of Rab-GTP turnover in the presences of both a GEF and GAP unlike the single molecule expulsion assay with mant-GDP.

Vps21 was incubated with appropriate buffers and assay components necessary to monitor phosphate release including the GAP Gyp1 and the GEF Vps9. Free ubiquitin was also added in order to determine if induced dimerization of Vps9 altered its catalytic activity. As seen in Figure 0-7, free ubiquitin did not substantially alter the kinetics of the reaction.

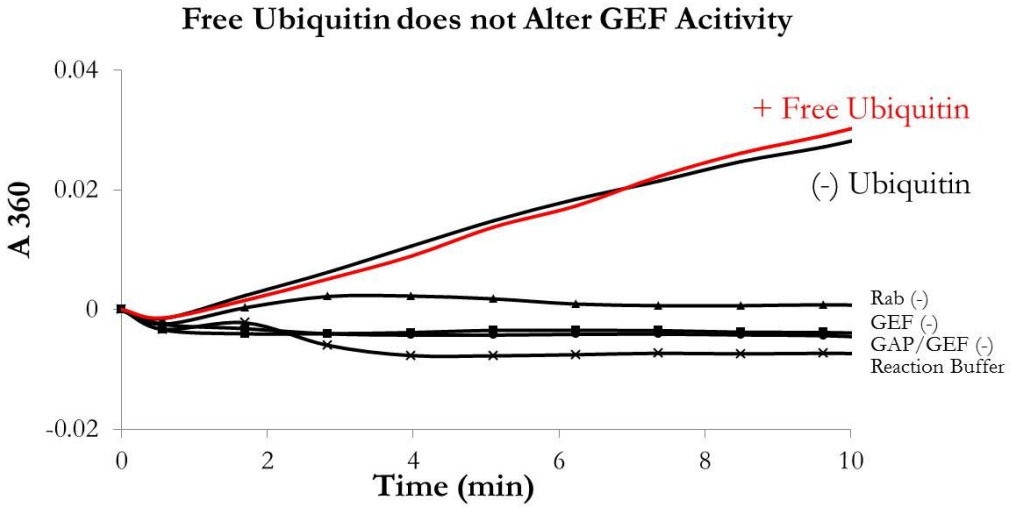

Figure 0-7 The presence of free ubiquitin does not drastically alter Vps9 catalytic GEF activity. Vps21 catalysis was measured with free ubiquitin (red) and without free ubiquitin (black). Controls lacking protein (x), lacking Vps21 (triangle), lacking Vps9 (square), and lacking both GAP and GEF (circle) show no phosphate release.

Interaction of Vac1 Domains with Vps21 via Y2H

Since both *in vitro* assays examining the effects of ubiquitin on the catalytic rates of Vps9 did not show large differences, I began examining the hypothesis that the CUE domain functions to localize Vps9 to Rab5 positive membranes. In order to do this I attempted to create an assay to quantify active Vps21-GTP *in vivo*. Similar assays have been developed for other small G-proteins (e.g. Cdc42, Arf1, Rab5a-c) and function on a related principle. Briefly, effector molecules and complexes are recruited only when active Rab-GTP is present and as such bind more tightly to the activated Rab complex. Pull-down assays utilizing immobilized effector molecules have proven useful in isolating active small G-proteins from cell lysates in order to quantify the ratio of active to inactive G-proteins. The effector molecules Vac1 (a.k.a. Vps19) was chosen due to its known role as a Vps21 effector and the large enhancement in binding to active versus inactive alleles of Vps21 in yeast-two-hybrid assays. Vac1 has proven difficult to work with as a full-length protein so I employed a Y2H assay to determine which domains of Vac1 were essential for binding Vps21-GTP. I examined eight Vac1 domain truncation constructs in order to determine the minimal interaction motif necessary

to bind Vps21-GTP (Figure 0-8). As shown in Figure 0-9, the second FYVE domain and C-terminal coil-coiled domain of Vac1 appears to be sufficient for Vps21 interaction.

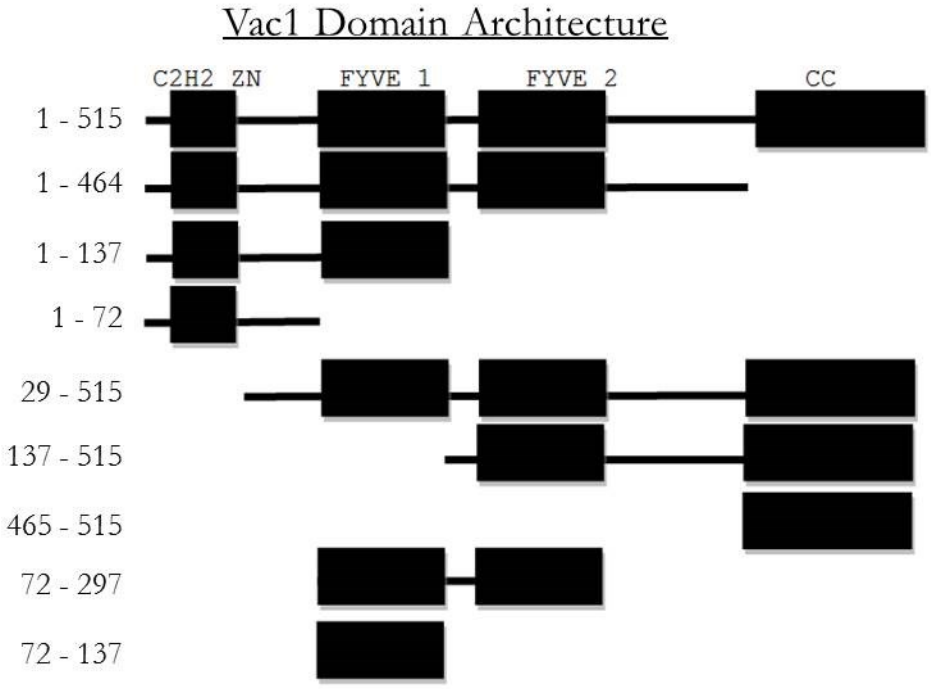

Figure 0-8 Vac1 Domain Map. Vac1 contains four identifiable domains: a C_2H_2 zinc finger, two central FYVE domains, and a C-terminal coiled-coil domain. Domain truncations were cloned into the pOBD2 yeast-two-hybrid bait vector in order to examine individual domain interactions with Vps21 and other endocytic genes.

Effector Pull-down Assay for Quantification of *In vivo* Vps21-GTP

A minimal FYVE-coiled-coil (FYVE-CC) domain was then expressed and purified with an N-terminal MBP epitope. Following purification, MBP-Vac1$_{FYVE\text{-}CC}$ was immobilized on amylose resin and incubated with either Vps21-GDP or Vps21-GTP. Unfortunately neither complex differentially bound to the immobilized Vac1 (Figure 0-11). Similar pull-down experiments were also performed using crude cell lysates, either wild-type or expressing constitutively active (Q66L) or inactive (S21N) forms of Vps21. Similar to the pull-down experiments with recombinant Vps21, the Vac1 fragment tested was unable to differentially retain the Q66L or S21N forms of Vps21(Figure 0-11).

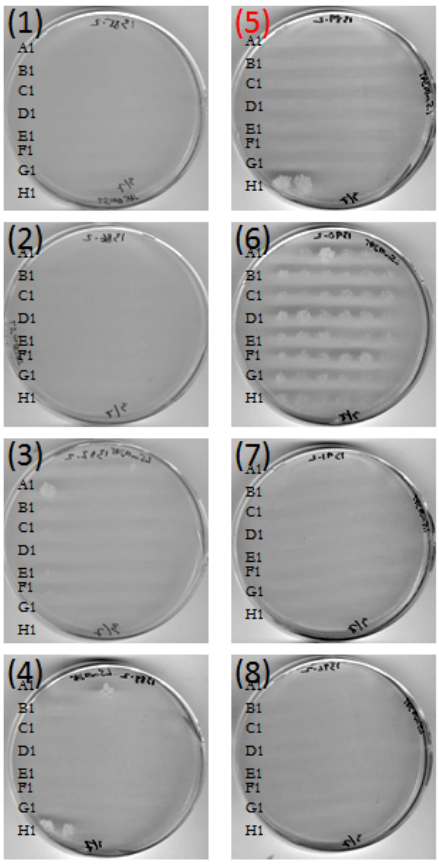

Loc.	Gene	Loc.	Gene
A1	Gga1	E1	Vps9 WT (1-322)
A2	Gga2	E2	Vps9 WT (1-205)
A3	Atg17	E3	Vps9 WT (206-322)
A4	Rsp5	E4	Vps9 WT (323-408)
A5	Sna3	E5	Vps9 WT (409-451)
A6	Yif1	E6	Vps9 WT (206-451)
B1	Yip1	F1	Ubiquitin
B2	Yip5	F2	Ypt1
B3	Mon1 (1-159)	F3	Sec4
B4	Mon1	F4	Ypt6
B5	Ccz1 (1-178)	F5	Ypt7
B6	Ccz1	F6	Ypt7 LB (D129N)
C1	Gyp7	G1	Ypt7 LB (T22N)
C2	Gyp1	G2	Ypt7 (K 5,6,48,56,140,147 R)
C3	Vps19 (1-465)	G3	Ypt10
C4	Vps19 (1-464)	G4	Ypt11
C5	Vps19 (1-137)	G5	Ypt31
C6	Vps19 (1-71)	G6	Ypt32
D1	Vps19 (30-515)	H1	Vps21
D2	Vps19 (138-515)	H2	Vps21-GTP (Q66L)
D3	Vps19 (465-515)	H3	Vps21-GDP (S21N)
D4	Vps19 (72-297)	H4	Ypt52
D5	Vps19 (72-137)	H5	Ypt53
D6	Vps9 WT (1-451)	H6	pOAD (-control)

Figure 0-9 Yeast-two-hybrid assays with Vac1 (Vps19) domain truncations. (A) Yeast-two-hybrid results for Vac1 domains against a prey library of endocytic genes. Domain truncations (4) $Vac1_{29\text{-}515}$ and (5) $Vac11_{37\text{-}515}$ showed interaction with constitutively active Vps21 mutant Q66L. (B) Map of Y2H bait library.

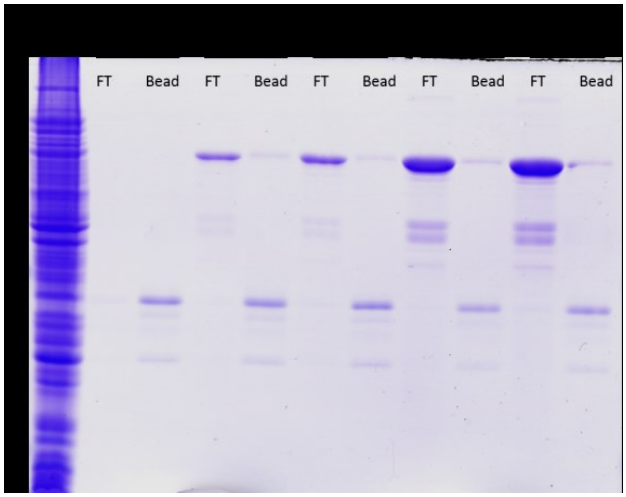

Figure 0-11 Affinity immobilized Vac1 domain does not interact with recombinant Vps21 loaded with either GTP or GDP. MBP-Vac1137-515 was bound to amylose resin and Vps21 was loaded with either GDP or GTP. Vps21 nucleotide states were incubated with loaded resin and unbound material was collected (FT). Resin was extensively washed and boiled with SDS loading buffer (Bead). Lanes 4-7 were loaded with with 1 uL of reaction, Lanes 8-11 were loaded with 10 uL of reaction.

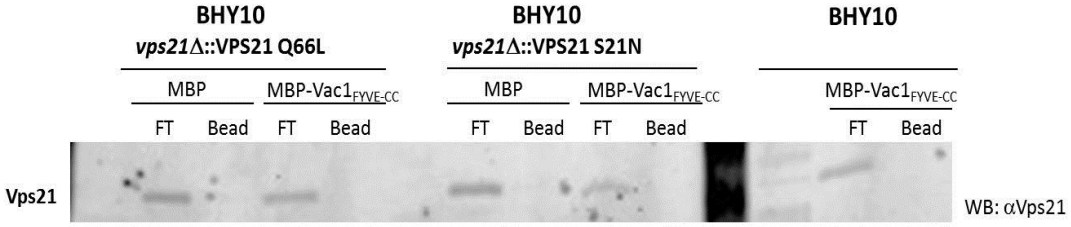

Figure 0-10 Affinity immobilized Vac1 domain (FYVE-CC) does not interact with Vps21 constitutively active (Q66L) or inactive (S21N) mutants from whole cell lysate. Yeast expressing constitutively active Vps21 Q66L, inactive Vps21 S21N, or WT Vps21 were lysed and crude cell lysate was incubated with either MBP or MBP-Vac1137-515 bound to amylose resin. Unbound fractions were collected (FT) and the resin was extensively washed. Bound material was collected by boiling with SDS loading buffer (Bead). Samples were analyzed by immunoblot against Vps21.

Discussion

One of the predominant hypothesis surrounding Vps9 function lies in the CUE domain interaction with ubiquitin. This high affinity interaction between the tri-helical CUE domain, which dimerizes around a single ubiquitin moiety, may be sufficient to bring Vps9 in proximity to Vps21-GDP on ubiquitin-decorated endosomes. There are multiple examples of GEF regulation and regulation via localization has long been hypothesized. Recent evidence with

Rabex-5, the mammalian endosomal GEF, shows that directed mistargeting of the GEF can induce cognate Rabs to mislocalize with their GEF [74]. If localization is a key determinant for Vps9 activity as has been hypothesized, then we would expect Vps9 CUE domain mutations which abolish ubiquitin binding, and presumably localization to ubiquitin-positive membranes, to display endocytic trafficking defects. It has previously been shown that mutations in the conserved 'MFP' sequence in the Vps9 CUE domain are null for both ubiquitin binding and Vps9 ubiquitylation [68]. Using the previously characterized F420A CUE mutation, I examined localization via microscopy and differential centrifugation. Microscopy of Vps9 F420A is shown as largely cytosolic, similar to wild type Vps9 (Figure 0-1). This was surprising since most models of Vps9 focus on its recruitment to endosomes via the CUE domain. It is unclear why Vps9 does not localize to endosomal puncta, either via microscopy or differential centrifugation. Experiments inhibiting deubiquitinases via N-ethylmaleamide were largely in agreement, suggesting deubiquitination during cell processing had little effect on localization. One reason may be that the amount of Vps9 in the cell is large enough to mask any obvious endosomal localization. Experiments using differential centrifugation to examine Vps9 localization are largely in agreement with microscopy studies (Figure 0-4). Both experiments show that the F420A ubiquitin null mutation has no effect on Vps9 localization. In Chapter 3, I demonstrate that Vps9 does become trapped on Class E compartments, which appear as large puncta adjacent to the vacuole limiting membrane. These compartments can be considered failed MVBs, and are commonly seen in deletions of various ESCRT subunits.

Previous cryo-electron microscopy images with *vps9*Δ null mutants show relatively normal vacuole morphology but with small endosomal honeycomb structures appearing in a fraction of the population. Our fluorescence microscopy shows that Vps9 CUE mutants have relatively normal endosomal and vacuole morphology (Figure 0-4). ALP and CPY are both expressed as pre-proteins, and are only cleaved to their final active forms upon entry into the vacuole lumen. As discussed in Chapter 1, CPY is first trafficked to endosomes, where it passes through the multivesicular body before fusing with the vacuole. ALP follows a separate pathway, where it traffics directly from the trans-Golgi to the vacuole, bypassing the endocytic network entirely. Defects in either CPY or ALP traffic are revealed by the presence of their uncleaved zymogen forms when visualized by western blot. As can be seen in Figure 0-4, CPY and ALP are both processed normally indicating that ubiquitin null mutation of Vps9 does not impair either trafficking pathway.

The VPS9-domain in both Rabex5 and Vps9 is more active when in isolation, rather than when expressed in either full length protein [72]. This has led to the speculation that these GEFs may possess self-regulatory features. The discovery that each protein can both bind ubiquitin and become ubiquitylated furthered this hypothesis, with theories leaning toward the sequestration of the ubiquitin binding domains via ubiquitin modification. However, it remained

unclear if modification of Vps9 with ubiquitin was simply a regulatory feature via appropriation of the CUE domain or if this modification directly altered the catalysis of Vps9. In order to examine this question, I expressed and purified mono-ubiquitylated Vps9 and tested its catalytic GEF activity *in vitro*. Single turn-over experiments were performed with Vps21 loaded with mant-GDP, a nucleotide analog which is only fluorescent while bound to the Rab. The induced expulsion of this florescent nucleotide via Vps9 resulted in decreased signal as seen in Figure 0-6B. Treatment with mono-ubiquitylated Vps9 did not appear to alter its catalytic activity. This indicates that while ubiquitylation of Vps9 may be playing an important regulatory feature in the cell, it is not doing so by altering the catalytic activity of Vps9 to activate Vps21.

Structural studies of the Vps9 CUE domain revealed how this domain was able to bind ubiquitin with relatively high affinity [38]. The Vps9 CUE domain has a low-affinity monomeric binding surface for ubiquitin, similar to other CUE domains. However, the tri-helical CUE domain can open as when dimerized, effectively sandwiching the bound ubiquitin between two binding surfaces, increasing its contact with ubiquitin, and therefore increasing the affinity.

We theorized that free ubiquitin could induce dimerization of Vps9 and possibly enhance its catalytic activity towards Vps21. A Rab G-protein multiple turn-over assay was used to examine this. In contrast to measurements with mant-GDP, this assay employs normal GTP nucleotide and assays the generation of inorganic phosphate released as GTP is hydrolyzed. This relies on several turn-over events of the Rab G-protein, using both GAP and GEF to catalyze GTP hydrolysis and GDP release, respectively. As shown in Figure 0-7, the presence of free ubiquitin did not alter the catalytic activity of Vps9 toward Vps21. While this assay failed to directly address if our recombinant Vps9 was in fact dimerizing with the free ubiquitin, previous studies have demonstrated Vps9 interaction with free ubiquitin to be robust [67].

Since these *in vitro* studies did not show any alterations on the catalytic activity of Vps9, we wanted to examine the quantity of active Vps21-GTP *in vivo*. Several methods have been developed to examine the active state of other small G-proteins *in vivo*. These generally involve using a domain of a downstream effector molecule which is known to strongly bind the active state of the G-protein. The Vps21 effector Vac1 was chosen since it has been shown to bind the constitutively active Vps21 Q66L mutant with high affinity with little binding towards the inactive Vps21 S21N mutant. The minimal domain for this interaction was mapped using Y2H to the second FYVE domain and C-terminal coiled-coil domain (Figure 0-9). This domain was then expressed and used to pull down pre-loaded Vps21-GDP or –GTP as well as incubated with cell lysate expressing constitutively active (Vps21 Q66L) and inactive (Vps21 S21N) alleles of

Vps21. It is unclear why neither of these pull downs showed interactions with Vps21 GTP. It is possible that other domains of Vac1 are necessary for a robust interaction via pull down.

Materials and Methods

Cloning and Strain Construction

Strains and plasmids are summarized in Table 1. Vps9 was cloned into pRSF H_6MBP via restriction digest. The Vps9 F420A mutant was created via QuikChange. Vectors were sequence-verified prior to use.

Yeast Two Hybrid, Culture, and Media

Cultures of the yeast prey library were decanted into 96-well plates and incubated with yeast expressing various Vac1 bait plasmids. Cultures were mixed and stamped onto YPD+Adenine (YPAD) and incubated at 30º C overnight. Mating plates were then replica plate d onto YPAD plates lacking leucine and tryptophan and incubated at 30º C for two days. YPAD plates were then replica plated onto YPAD-trp-leu plates containing 1.5 mM 3-AT and incubated at 30º C for 5 days.

Protein Purification

GST-Vps19, H_6MBP-Vps21, H_6-Uba1, H_6-Ubc4, H_6-Ubc5, GST-Rsp5, H_6-Ubiquitin, H_6MBP-Vps9 (WT and F420A) were expressed individually in BL21(DE3) cells. Briefly, 1 L of Terrific Broth was inoculated with overnight culture and grown at 37º C, 225 rpm to an OD600 ~0.8. Culture was induced with 100 μM IPTG and allowed to express for 5 hours. Cells pellets were generated at 5,000 x *g* and frozen at -20º C until purification.

Cell pellets were thawed and lysed in Phosphate Lysis Buffer (PLB) via four passes through a cell homogenizer. Insoluble material was removed by centrifugation at 20,000 x*g* for 30 min. Soluble material was incubated with appropriate resin (Ni-NTA, Glutathione, Amylose) at 4º C for 2 hours. Each resin was washed with 10 column volumes of PLB and eluted in PLB with appropriate small molecules (300 mM imidazole, 20 mM glutathione, 10 mM maltose). Material was dialyzed overnight in PLB, concentrated, and flash frozen in liquid nitrogen. Proteins were stored at -80º C until used.

In Vitro Ubiquitylation of Vps9 and Purification

15 μM H_6MBP-Vps9 was thawed and incubated with 0.1 μM Uba1, 1.5 μM Ubc4, 1.5 μM Ubc5, 2 μM Rsp5, 1705 μM H_6-Ub, and reaction buffer (50 mM Tris-Cl, pH 7.5, 2 mM ATP, and 3 mM $MgCl_2$) at 30º C for 2 hours. Reactions were then incubated with equilibrated amylose resin (New England Biolabs) for 1 h at 4º C. The amylose beads were washed twice with 10 mL of reaction buffer and eluted with 20 mM maltose in reaction buffer. Eluate was then incubated with 6 μg of TEV protease overnight at 4º C. Ni-NTA resin (Amersham Biosciences) was equilibrated with 50 mM Tris-Cl, 7.5, 300 mM NaCl, and 1 mM DTT. Resin was incubated with overnight TEV digests for 1 h at 4º C, washed five times with equilibration buffer, and eluted with increasing amounts of imidazole (20 – 500 mM). Fractions were examined by SDS-PAGE to confirm separation of ubiquitylated and unreacted Vps9. Vps9-Ub fractions were then pooled and run over a Superdex-200 sizing column (GE Healthcare) in Ni-NTA equilibration buffer above to separate Vps9-Ub and contaminating affinity tag. 30 pmol of Vps9-Ub was then incubated with 0.4 μM Usp2cc for 1 h at 30º C and analyzed by SDS-PAGE.

In Vitro GEF Assay – mantGDP Expulsion

38 pmol Vps9-Ub was incubated with 2 nmol Usp2cc at 37º C for 1 h and the reaction was then polished on a Superdex-200 column to remove Usp2cc and free Ubiquitin. Reaction buffer (50 mM Tris-Cl, pH 7.5, 100 mM NaCl, 5 mM $MgCl_2$, 5 mM DTT), 5 μM GTP, and 100 nM Vps21 (pre-loaded with mantGDP) was monitored for 200 sec to establish a baseline. 100 nM Vps9-Ub or Vps9-Ub treated with Usp2cc (above) was added and fluorescence at 440 nm was measured every 1 sec for 1200 sec.

In Vitro GEF Assay – Phosphate Release

Aliquots of $Gyp1_{1\text{-}46}$, Vps9, Ubiquitin, and Vps21 were thawed and their concentrations determined using a Bradford assay. Enzymatic reactions containing reaction buffer (20 mM HEPES, pH 7.5, 150 mM NaCl, 10 mM $MgCl_2$, 0.15 mM MESG, 0.75 U/mL PNP, and 0.2 mM GTP), 1.5 μM $Gyp1_{1\text{-}46}$, 3 μM Vps9, 70 μM Ubiquitin, and 23 μM Vps21 were monitored at 360 nm for 1 h in a Victor3 Fluorescent Plate Reader (Perkin Elmer).

Microscopy

Fluorescence microscopy was performed with an Olympus IX71 light microscope, an EMCCD (Andor Ixon) camera, Pl 60× NA 1.45 or 100× NA 1.3 objectives, and appropriate filter sets. Andor IQ v.6.0.3.62 (Andor Bioimaging, Nottingham, UK) software was used for data collection. Image/J v.1.45s (J. Rasband, U.S. National Institutes of Health

http://rsb.info.nih.gov/ij/). For imaging of mCherry-Vps9, yeast cells were grown overnight in selective defined media at 30° C and diluted to OD_{600nm} 0.2 the following morning. 1.5 mL of culture was harvested at mid-log phase (~0.5 - 0.7 OD600nm) by sedimenting at 3,000 × g for 3 min., and half was suspended in 100 μL fresh media containing 50 μM FM 4-64 styryl dye (Invitrogen). Cells were incubated for 15 min. at room temperature, centrifuged for 5 min. at 3,000 × g, and suspended in 1 mL of fresh media and incubated at 30° C for 1 h. Suspensions were then centrifuged at 3,000 × g, suspended in 50 μL fresh media and imaged as described above.

Subcellular Fractionation

Subcellular fractionation of yeast cell extracts was performed by modifying a previously described protocol (Angers et. al., 2009). Clarified yeast cell lysates were prepared. Briefly, yeast were grown in YPD at 30º C to OD600 ~1.0. Cells were harvested by centrifugation and washed in 100 mM Tris-Cl, pH 9.4 and 10 mM β-mercaptoethanol for 10 min. at room temperature. Cells were sedimented and incubated in spheroplasting buffer (1 M sorbitol, 50 mM Tris-Cl, pH 7.9, and 8% YPD) with lyticase at 30º C for 25 min. Spheroplasts were suspended in yeast lysis buffer (20 mM HEPES-KOH, pH 6.8, 200 mM sorbitol, 2 mM EDTA, 50 mM potassium acetate, and appropriate protease inhibitors) and lysed with 30 strokes in a Dounce homogenized. Clarified cell lysates were then produced by sedimenting unlysed cells at 1000 x g for 5 minutes. Clarified yeast cell lysates were then sedimented at 13,000 x g for 15 min. to obtain P13 (pellet) and S13 (supernatant) fractions. The S13 fraction was then centrifuged at 100,000 x g for 45 min. to obtain P100 (pellet) and S100 (supernatant) fractions. The two pellets were gently resuspended in equivolume lysis buffer. The whole cell lysates and other fractions were loaded onto SDS-PAGE and subjected to Western blot analysis.

GST Pull downs

To prepare GST-affinity ligand resin, 1 mL of BL21 (DE3) cells expressing GST-fusion protein were thawed, lysed by sonication, and centrifuged at 20,000 x g for 20 min. 500 μL of the clarified lysate was added to 50 μL of glutathione sepharose 4B (Amersham Biosciences, Piscataway, NJ) beads pre-washed with PBS. After binding overnight at 4º C on a nutator, the beads were washed with PBS, PBS + 300 mM NaCl, and yeast lysis buffer. Vps21 aliquots were thawed and loaded with indicated nucleotide. Briefly, ~ 60 μg of Rab was incubated with 5 mM EDTA and 2 mg nucleotide for 1 hour at room temperature. Loading was quenched with excess magnesium chloride and buffer exchanged using a micro-spin column (BioRad GF Spin Column) into lysis buffer. Nucleotide loaded Rab was then

incubated with 50 μL beads for 2 hour at 4° C. After binding the beads were washed with lysis buffer and analyzed by SDS-PAGE.

Discovery of Muk1: A Novel VPS9-Domain Containing Protein

Introduction

The Rab5 family coordinates events essential in endolysosomal traffic, including endosome maturation and targeting of Golgi-derived vesicles to early and late endosomes. The Rab7 family resides on late endosomal or vacuolar membranes and controls hetero- and homotypic fusion events at these organelles. Like humans, S. cerevisiae harbors three Rab5 isoforms (Vps21, Ypt52, and Ypt53) and one Rab7 (Ypt7). Disruption of Vps21 results in obvious endolysosomal trafficking and morphology phenotypes, while Ypt52 and Ypt53 are partially redundant with Vps21 [55; 75-77]. In addition, recent work implicates Ypt53 in cellular stress responses [77].

Rab signaling is regulated through the binding of GDP and GTP. Rabs adopt an 'active' conformation when GTP-bound, allowing them to bind and coordinate activities of effector molecules required for vesicle docking and fusion. Intrinsic rates of Rab GTP hydrolysis and GDP dissociation are slow; Rabs rely on regulatory proteins to catalyze transitions between the active and inactive states. Rab signaling is promoted by guanine nucleotide exchange factors (GEFs) which stimulate GDP release, allowing GTP to bind. G-protein-accelerating proteins (GAPs) terminate Rab signaling by triggering GTP hydrolysis. Rabs are anchored to membranes through a pair of prenylated cysteines at their C-termini. A chaperone, GDP dissociation inhibitor (GDI), can extract bis-prenylated Rab-GDP from membranes, and can deposit the bound Rabs back onto specific membranes through a mechanism that is accelerated by GDI-displacement factors (GDFs) [78-80].

As described in Chapter 1, GEF domains are highly specific toward Rab subfamilies. The VPS9-domain was identified in S. cerevisiae Vps9 and H. sapiens Rabex-5; both proteins were shown to stimulate GDP release on G proteins of the Rab5 family [15; 59]. The mammalian Rin proteins (Rin1-3) also contain VPS9-domains and act as GEFs against Rab5 isoforms, suggesting that VPS9-domains generally function to stimulate signaling by members of the Rab5 family [81-83]. VPS9-domain proteins localize to appropriate membranes by interacting with a variety of targeting determinants. For example, yeast Vps9 has a CUE domain that is believed to bind ubiquitylated cargo molecules at the endosome surface. Similarly, mammalian Rabex-5 has an ubiquitin binding domain and it also interacts with an array of accessory proteins. In contrast, mammalian Rin1 interacts selectively with internalized EGFR receptors to promote their endosomal down-regulation.

At least 22 mammalian proteins have VPS9-domains; two S. cerevisiae proteins contain intact VPS9-domains: Vps9 and Muk1 (coMpUtationally-linked to KAP95) [84]. Using biochemical and genetic analyses, we now show that

Muk1 is a specific GEF for yeast Rab5 proteins, and that its *in vivo* function is partially redundant with the major GEF of the Rab5 family, Vps9.

Results

Growth phenotypes of Muk1 deletion and overexpression in cells lacking Vps9

The three Rab5 paralogs of budding yeast (Vps21, Ypt52, and Ypt53) are partially redundant, with single mutants of Vps21 displaying clear sorting and morphology phenotypes that are further enhanced by deletion of Ypt52, Ypt53, or both [55; 77; 85]. At 30º C *vps21*Δ *ypt52*Δ double mutants had delayed entry into log phase (**Figure 0-1**A) and had severe growth defects when subjected to ionic or thermal stress (**Figure 0-1**B,C). Almost identical growth defects were observed with *vps21*Δ *ypt52*Δ *ypt53*Δ triple mutants [55; 77]. In marked contrast, single mutants lacking Vps9 grew almost normally when grown on solid or liquid media (**Figure 0-1**). Together, these results suggested that residual Rab5 signaling occurs in the absence of Vps9.

Because Muk1 contains a VPS9-domain [73], we hypothesized that Muk1 drives the residual Rab5 signaling presumed to occur in *vps9*Δ deletion mutants. If this were the case, a *vps9*Δ *muk1*Δ double deletion should phenocopy the severe growth and trafficking defects of the *vps21*Δ *ypt52*Δ double mutant. As shown in Figure 0-1, we observed nearly identical growth delays and defects in both Rab5 null (*vps21*Δ *ypt52*Δ and GEF null (*vps9*Δ *muk1*Δ strains. Moreover, expression of MUK1 from a high-copy plasmid largely suppressed the growth defect of a *vps9*Δ single mutant at 37° C (Figure 0-1C). Hence, MUK1 and VPS9 are partially redundant in conferring cellular tolerance of thermal stress, and loss of both MUK1 and VPS9 phenocopies the growth defects of mutants mostly or completely lacking Rab5.

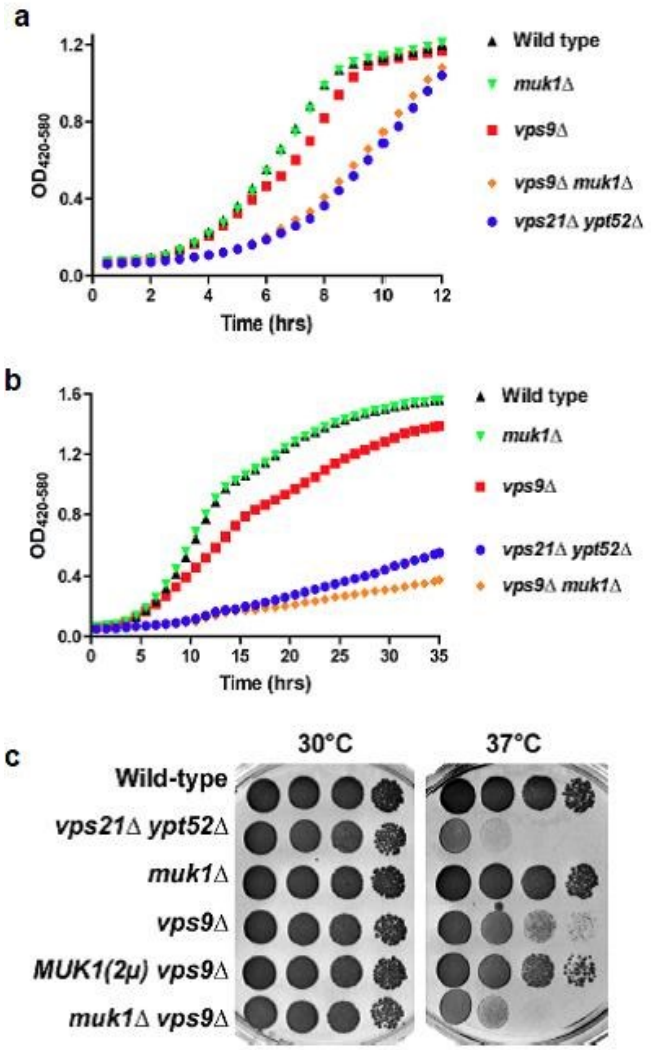

Figure 0-1 A dual GEF deletion mutant phenocopies severe Rab5 deficiency. (A and B) Growth curves at 30°C in YPD liquid media (A) and media supplemented with 200 mM CaCl2 (B). Data points each represent the mean of 8 replicate samples. (C) Limiting dilution growth assay on YPD agar plates at 30°C and 37°C. Muk1, under native promoter and terminator, was overexpressed on a high copy (2□) plasmid.

We next asked whether Muk1 and Vps9 cooperate in endolysosomal biogenesis and cargo trafficking. Carboxypeptidase Y (CPY), a soluble vacuolar hydrolase, traffics from the Golgi to the prevacuolar endosome by binding the CPY receptor Vps10, which cycles between these compartments. Perturbation of Vps10 traffic results in CPY secretion, which can be monitored with the chimeric reporter CPY-invertase [86]. Wild-type cells secrete little CPY-invertase, *vps21*Δ or *vps9*Δ single mutants secrete similar, substantial amounts of CPY-invertase, and *vps21*Δ *ypt52*Δ double mutants secrete roughly twice as much CPY-invertase as either *vps21*Δ or *vps9*Δ single mutants [77]. Like wild-type cells, *muk1*Δ single mutants exhibited no detectable CPY-invertase mistargeting. In marked contrast, *vps9*Δ *muk1*Δ double mutants mistargetted CPY-invertase just as severely as *vps21*Δ *ypt52*Δ double mutants (Figure 0-1).

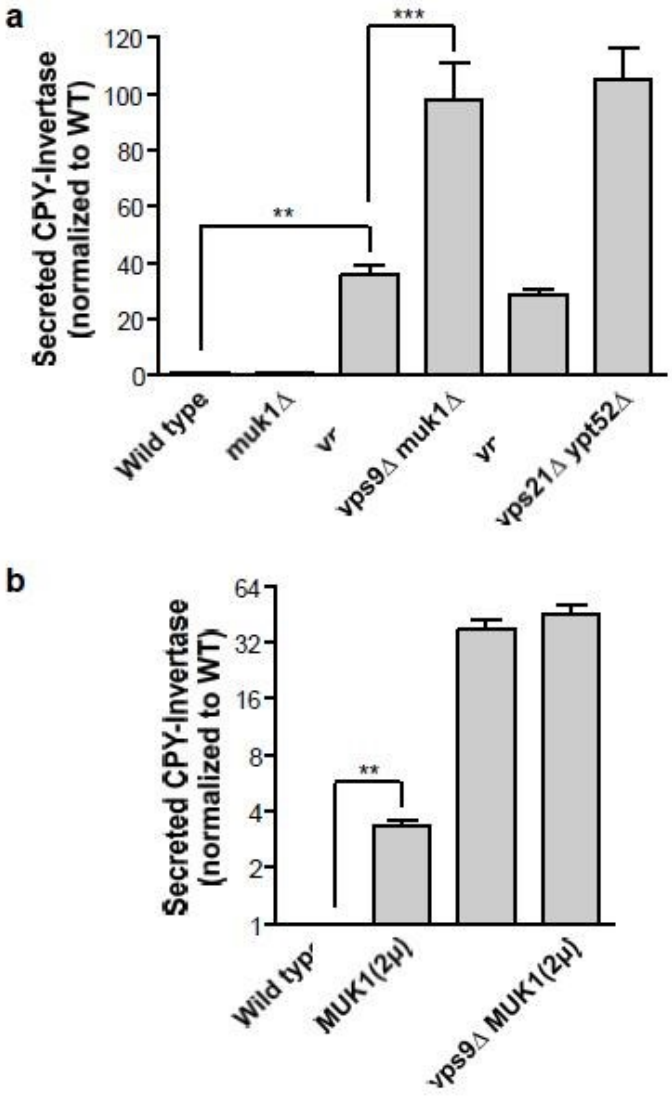

Figure 0-2 Redundant and non-redundant functions of Vps9 and Muk1 in CPY targeting. (A and B) Measurement of extracellular CPY-invertase normalized to wild-type. Bar graphs show means ± S.E.M. of 4 independent experiments. In (A), paired one-way ANOVA: p<0.0001 overall; ***, p<0.001; **, p<0.01. All pairwise comparisons are statistically significant, except wild type vs. muk1Δ, vps9Δ vs. vps21Δ, and vps21Δ ypt52Δ vs. vps9Δ muk1Δ. In (B), ** p=0.0034, paired, two-tailed t-test.

Unlike the cell growth assays (Figure 0-1C), Muk1 overproduction did not suppress CPY mistargeting in a *vps9*Δ background (Figure 0-2B). In fact, Muk1 overproduction in wild-type cells caused a mild but statistically significant CPY mistargeting phenotype (Figure 0-2B). Taken together, these experiments suggest that Vps9 and Muk1 have both overlapping and distinct functions within the Golgi-endosome network.

Muk1 deletion exacerbates MVB targeting defects in cells lacking Vps9

We recently demonstrated an absolute requirement for Rab5 signaling in the biogenesis and sorting functions of late endosomal multivesicular bodies (MVBs). *vps21*Δ *ypt52*Δ double mutants totally lack organelles with MVB architecture and mistarget cargo that is normally packaged into intraluminal vesicles (ILVs) at the MVB [77]. We predicted that if Muk1 operates in concert with Vps9 to activate Rab5, the rate and fidelity of MVB cargo transport should be impaired in *vps9*Δ *muk1*Δ double mutants, and perhaps in *muk1*Δ single mutants as well. To test these predictions we examined four representative transmembrane proteins that are targeted to ILVs: carboxypeptidase S (CPS) and Sna3, which traffic from the late Golgi to the MVB, and Mup1 and Ste3, which traffic from the plasma membrane to the MVB. As the following experiments show, all four MVB cargos are severely missorted in *vps9*Δ *muk1*Δ double mutant cells.

CPS targeting was monitored using a GFP-CPS fusion protein. Wild-type cells sort GFP-CPS into ILVs, which deliver GFP-CPS to the vacuole lumen when MVBs fuse with vacuoles. In cells with impaired MVB biogenesis or sorting, GFP-CPS is diverted onto the vacuole limiting membrane, or may become trapped in prevacuolar "Class E" endosomal compartments. Class E compartments appear as large puncta adjacent to the vacuole and are regularly observed in *vps4*Δ mutants [77]. Consistent with the CPY secretion results (Figure 0-2), *muk1*Δ cells correctly targeted CPS to the vacuolar lumen, while *vps9*Δ cells exhibited a partial CPS sorting defect (Figure 0-3). In *muk1*Δ *vps9*Δ double mutants CPS was mistargetted to the vacuolar limiting membrane and was also observed in prevacuolar endosomal compartments (Figure 0-3).

Fluorescence microscopy of cells expressing GFP-CPS (carboxypeptidase S). Note that in contrast to the *vps4*Δ Class E phenotype of CPS mislocalized to the vacuole limiting membrane and concentrated at large puncta adjacent to the vacuole, cells lacking Rab5 or Rab5 GEF functions display CPS mislocalized to the limiting membrane and distributed throughout the cytoplasm.

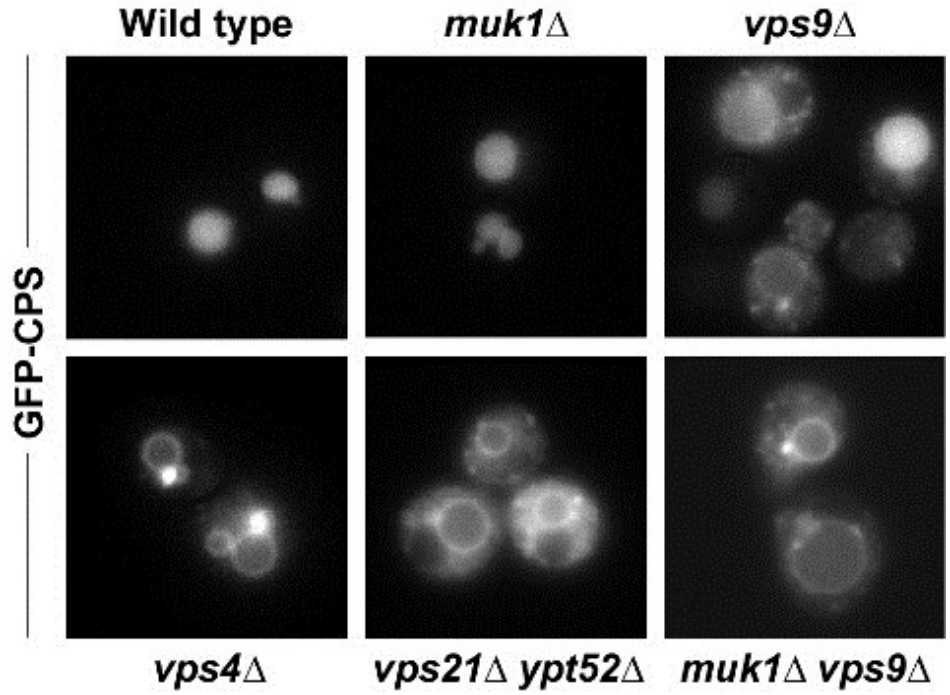

Figure 0-3 Biosynthetic traffic to the vacuole lumen in GEF null and Rab5-deficient mutants.

Like CPS, Sna3 traffics from Golgi to MVB, and is then deposited into the vacuole lumen. The fidelity of Sna3 luminal targeting is robust compared to other ubiquitin-dependent MVB cargoes, and Sna3 sorting is sometimes used as a proxy for luminal vesicle formation [33; 87; 88]. We observed Sna3 targeting by both fluorescence microscopy (also employing a vital stain, FM4-64, that labels vacuole membranes and upstream endocytic compartments) and a quantitative assay called LUCID (LUCiferase reporter of Intraluminal Deposition). LUCID is a ratio metric luciferase assay that monitors the sequestration of cargo into MVBs [77]. LUCID employs a soluble, control Renilla luciferase (RLuc) as well as an ILV cargo (in this case Sna3) fused to firefly luciferase (FLuc) at its cytosolic terminus. The ratio of FLuc to RLuc decreases as internalized Sna3-FLuc is sequestered into ILVs at the MVB (which are subsequently destroyed in the vacuole lumen) and away from its soluble substrate. We observed no discernible missorting of Sna3 in *muk1*Δ mutant cells, while *vps9*Δ mutants had an intermediate missorting phenotype somewhat more severe than a *vps21*Δ mutant. The double GEF mutant (*vps9*Δ *muk1*Δ) strongly missorted Sna3, on par with the double Rab5 mutant (*vps21*Δ y*pt52*Δ).

Sna3 is also strongly missorted in *vps4*Δ mutant cells. Like Rab5-deficient cells [77], *vps9*Δ *muk1*Δ double mutant cells accumulated Sna3 in puncta dispersed throughout the cytoplasm, rather than in a Class E prevacuolar compartment (Figure 0-4A). Similarly, in several previous studies[89-92] mistargetted Sna3 did not accumulate at the

vacuolar limiting membrane as was the case with mistargetted CPS (Figure 0-3).In contrast, when multiple Sna3 sorting motifs are simultaneously disrupted, including multiple cytosolic lysines and tyrosines, Sna3 does accumulate at the vacuole limiting membrane [89]. These results may indicate that mistargetted Sna3 can be retrieved from the vacuole. These findings suggest that *vps9*Δ *muk1*Δ double mutants have a defect distinct, and probably upstream, of the Class E compartment formed in cells lacking Vps4 or other proteins needed for ILV biogenesis [77].

Mup1, a high-affinity Met transporter, localizes to the plasma membrane in Met-limited media. At higher levels of extracellular Met Mup1 is rapidly endocytosed and trafficked through the MVB, en route to the vacuole lumen [93; 94]. As shown in Figure 0-5A, Mup1 localizes to the plasma membrane in both a *vps9*Δ and *muk1*Δ mutant with a small fraction accumulating in puncta at low Met levels. As with wild-type cells, Met exposure resulted in rapid and complete Mup1 internalization in a *muk1*Δ single mutant, while a *vps9*Δ mutant displayed residual Mup1 at the plasma membrane. Double mutant *vps9*Δ *muk1*Δ cells correctly targeted Mup1 to the plasma membrane and were competent to internalize Mup1 when exposed to Met. However, subsequent Mup1 trafficking through the endolysosomal system was severely disrupted, with Mup1 trapped in both intracellular punctate structures and on the vacuolar limiting membrane. There was no detectable Mup1 in the vacuole lumen (Figure 0-5A).

To quantify the kinetics of Mup1 delivery into MVBs, we monitored Mup1 traffic using a Mup1-LUCID reporter. We observed normal Mup1 trafficking in wild-type and *muk1*Δ single mutant cells. In contrast, *vps9*Δ, *vps21*Δ, or *vps4*Δ mutants had both elevated steady-state levels of Mup1 in the absence of Met, and severe defects in Mup1 targeting to the MVB when Met was added to the medium (Figure 0-5B). Double mutant *vps21*Δ *ypt52*Δ and *vps9*Δ *muk1*Δ cells were not analyzed in LUCID experiments due to their extremely slow growth in Met-limited synthetic media.

Ste3 is a G protein coupled receptor at the plasma membrane where it binds yeast a-factor to initiate the mating response. In the absence of mating factor it is constitutively internalized, packaged into ILVs at the MVB, and routed to the vacuole for degradation [90]. Cells without Vps4 entirely lack MVB intraluminal vesicles [95; 96]. Using Ste3-LUCID, *vps4*Δ mutants accumulated substantially more Ste3 than wild-type cells, while *vps9*Δ and *vps21*Δ mutants had somewhat less severe Ste3 accumulation. Cells lacking Muk1 had a small but statistically significant accumulation of Ste3 relative to wild-type cells (Figure 0-5). These results indicate that endocytic traffic to the vacuole generally tolerates loss of Muk1 without strong defects, but that Muk1 may contribute to efficient endocytic down-regulation or recycling of Ste3.

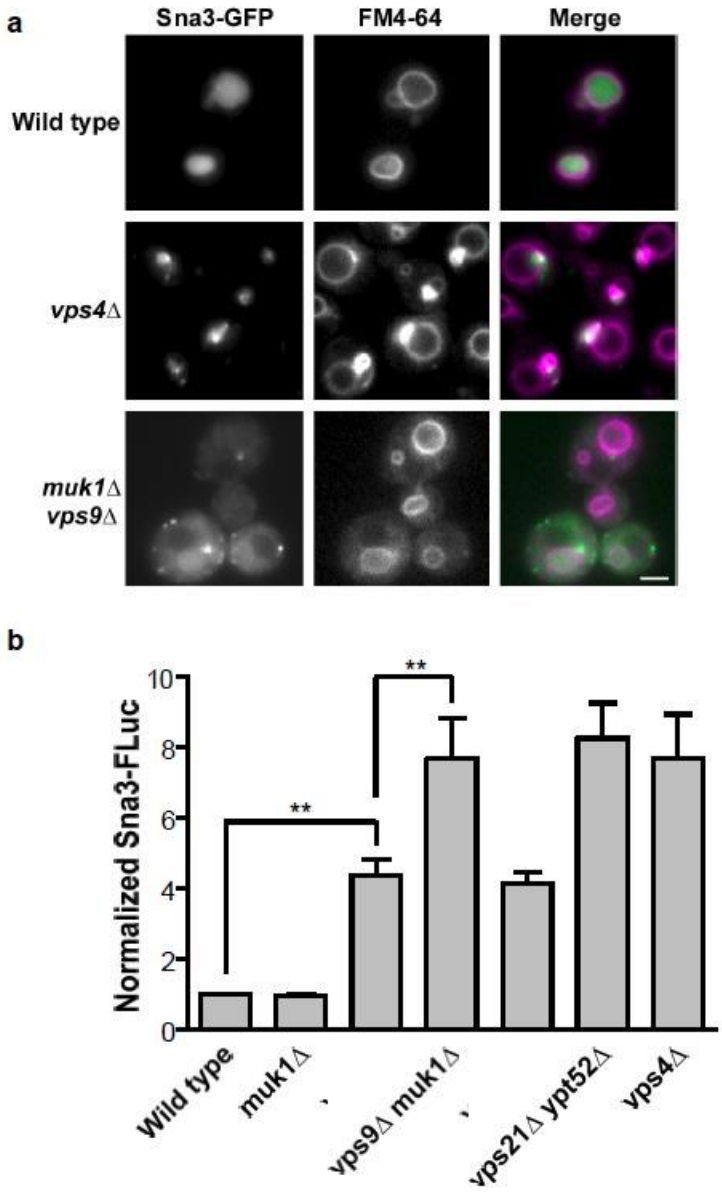

Figure 0-4 Biosynthetic traffic to the vacuole lumen in GEF null and Rab5-deficient mutants. (A) Fluorescence microscopy of cells expressing Sna3-GFP (green) and stained with the endocytic tracer dye FM4-64 (purple) that stains vacuole membranes. Note that while *vps4*Δ Class E mutants concentrate Sna3 at FM 4-64-stained perivacuolar puncta, *muk1*Δ *vps9*Δ cells mislocalize Sna3 at puncta throughout the cytoplasm. Scale bar = 2 μm. (B) Box plot presentation of 5 independent LUCID assays of Sna3-Fluc. Paired one-way ANOVA: p<0.0001 overall; ***, p<0.001, **, p<0.01 and *, p<0.05 compared to wild type. All pairwise comparisons are statistically significant, except wild type vs. *muk1Δ*, *vps9Δ* vs. *vps21Δ*, *vps21Δ ypt52Δ* vs. *vps9Δ muk1Δ*, *vps4*Δ vs. *vps21*Δ *ypt52*Δ, and *vps4*Δ vs. *vps9Δ muk1Δ*. LUCID, luciferase reporter of intralumenal deposition. FLuc, firefly luciferase.

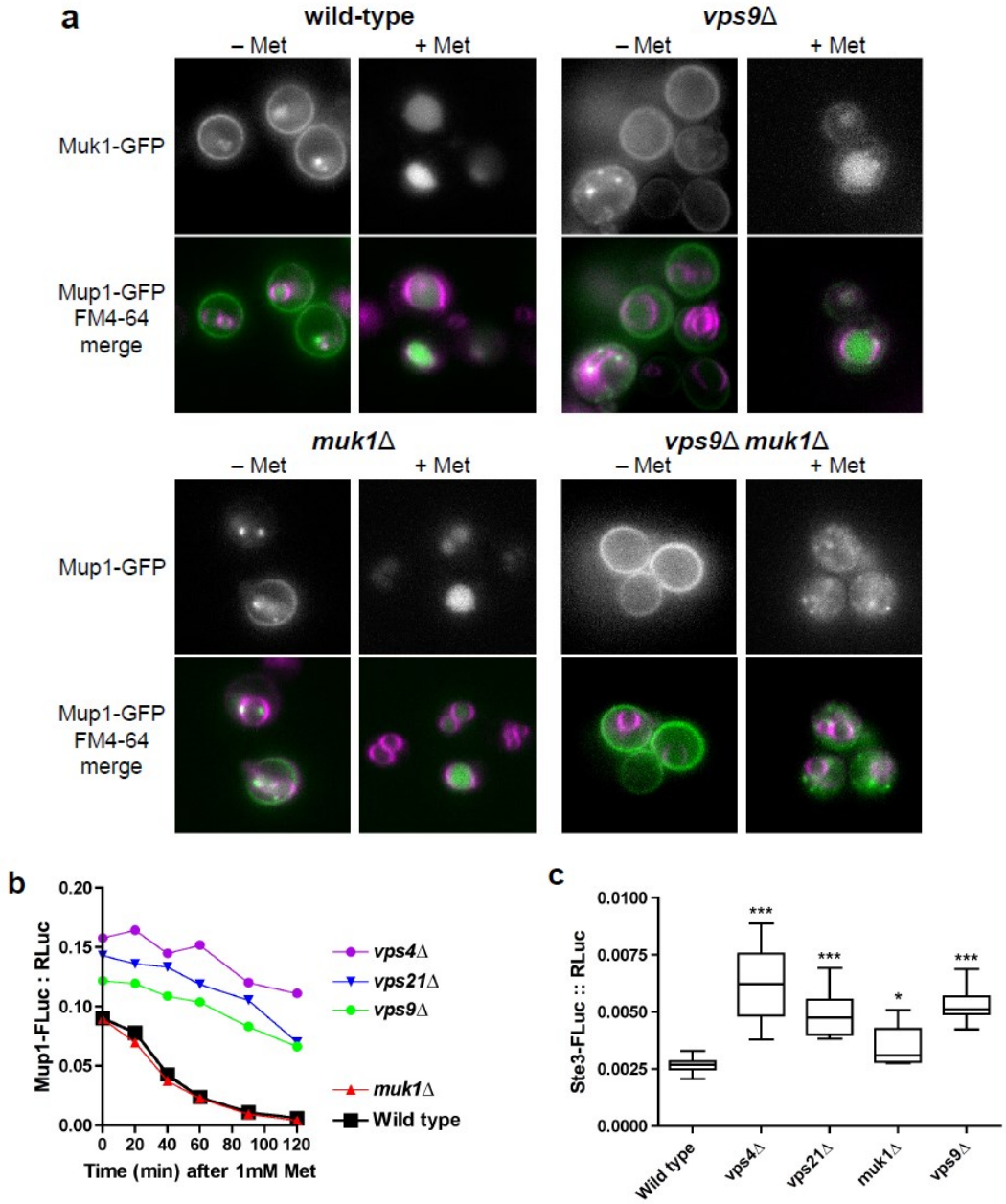

Figure 0-5 Endocytic traffic to the vacuole lumen in GEF null and Rab5-deficient mutants. (A) Mup1-GFP (green) was monitored by fluorescence microscopy in cells labeled with FM4-64 (purple) both in the absence of methionine (-Met) and 1 h after the addition of 1 mM methionine (+Met) to stimulate internalization of Mup1-GFP from the plasma membrane and transport to the vacuole lumen. (B) Time-course LUCID analysis of Mup1-FLuc down regulation after addition of 1 mM methionine. Points represent mean of two duplicate samples from a representative experiment. (C) LUCID analysis of Ste3-FLuc. Box plot summarizes 10 biological replicates pooled across three independent experiments. One-way ANOVA: $p<0.0001$ overall; ***, $p<0.001$ and *, $p<0.05$ compared to wild-type. (B and C) Mup1-FLuc and Ste3-FLuc were each normalized to a cytosolic RLuc (Renilla luciferase) loading control expressed from the same plasmid.

Muk1 is a GEF for Rab5 paralogs

We next assayed the GEF activities of purified recombinant Vps9 and Muk1 for various endolysosomal Rabs. In the presence of Gyp1TBC, a hydrolysis-accelerating GAP, Vps21-GTP and several other yeast Rabs undergo a single turnover of GTP hydrolysis [77; 91; 97]. In the presence of GTP and a GEF such as Vps9, GDP is exchanged and additional cycles of GTP hydrolysis can then occur [76]. In this reaction system, we measure GTP hydrolysis through evolution of inorganic phosphate, using a real-time spectrophotometric assay based on purine nucleoside phosphorylase (PNP) and MESG, a small molecule reporter which changes its UV absorbance when phosphorylated by PNP [97; 98].

As expected (Figure 0-6), Vps9 stimulated multiple cycles of GTP hydrolysis by Vps21, Ypt52, and Ypt53, but not on Ypt7, the vacuolar Rab. Muk1 exhibited a pattern of GEF activity similar to Vps9, stimulating multiple-cycle GTP hydrolysis on Vps21, Ypt52 and Yp53, but not on Ypt7. In combination with the genetic experiments described above, these experiments establish Muk1 as an authentic GEF with selectivity for Rab5 paralogs.

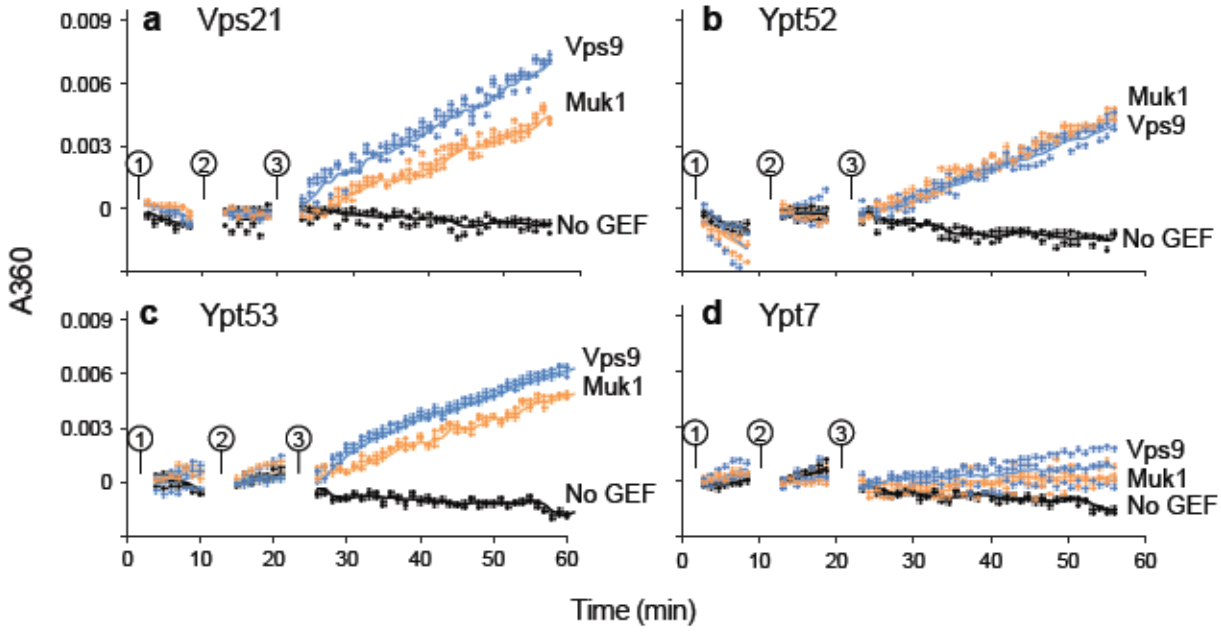

Figure 0-6 GEF activities of purified Vps9 and Muk1. Coupled GEF-GAP phosphate release assay with Vps9 (blue), Muk1 (orange), or No GEF (black) against (A) Vps21, (B) Ypt52, (C) Ypt53, and (D) Ypt7. Individual points show data from triplicate samples in a representative experiment. Lines show smoothed means. Reactions were monitored following (1) Rab and reaction buffer for 10 min., (2) addition of GAP for 10 min., and (3) addition of GEF for 1 h.

Muk1 and Vps9 Localization

To compare the localization of Vps9 and Muk1, we expressed GFP-Muk1 and mCherry-Vps9 fusion proteins. The tagged proteins were functional, as evidenced by their ability to rescue the heat stress sensitivity phenotype of

*muk1*Δ *vps9*Δ double mutant cells (Figure 0-7A). When observed in live cells, Vps9 is predominantly cytosolic with no discernible localization to specific subcellular structures. However, in a *vps4*Δ mutant, mCherry-Vps9 localizes to the prevacuolar "Class E" compartment, which is also highly enriched with Vps21 [99]. We therefore compared the localization of tagged Vps9 and Muk1 in wild type and *vps4*Δ mutant cells. Both GFP-Muk1 and mCherry-Vps9 were predominantly cytosolic in wild-type cells, but only mCherry-Vps9 redistributed to Class E compartment punctae in a *vps4*Δ mutant (Figure 0-7B).

To explore possible binding partners and help determine where Muk1 may be functioning we assayed Muk1 against a host of endocytic and other trafficking genes using yeast two-hybrid tests. As expected, Muk1 interacted with Vps21. Interactions with Ypt52 and Ypt53 were not detected, however our conditions for two-hybrid (single-copy vectors and 3-AT on the test plates) are relatively stringent. We also verified previously reported two-hybrid interactions with multiple trafficking proteins including Ypt6, a Rab that controls Golgi-Endosome transport, Exo84, a subunit of the plasma membrane Exocyst tethering complex, along with weak interactions with the vacuolar Rab Ypt7 and its GEF Mon1 [100]. Notably, all of these candidate interactors reside at the peripheral zones that delineate of the Rab5 signaling domain: the plasma membrane, the vacuole and the late Golgi. In addition, while Vps9 and mammalian Rabex-5 both comprise ubiquitin-binding domains, Muk1 lacks any motifs implicated in ubiquitin binding. We conclude that while Muk1 and Vps9 are both able to catalyze nucleotide exchange with all three yeast Rab5 proteins, the two yeast Rab5 GEFs possess distinct localization determinants and probably operate at distinct subcellular locations

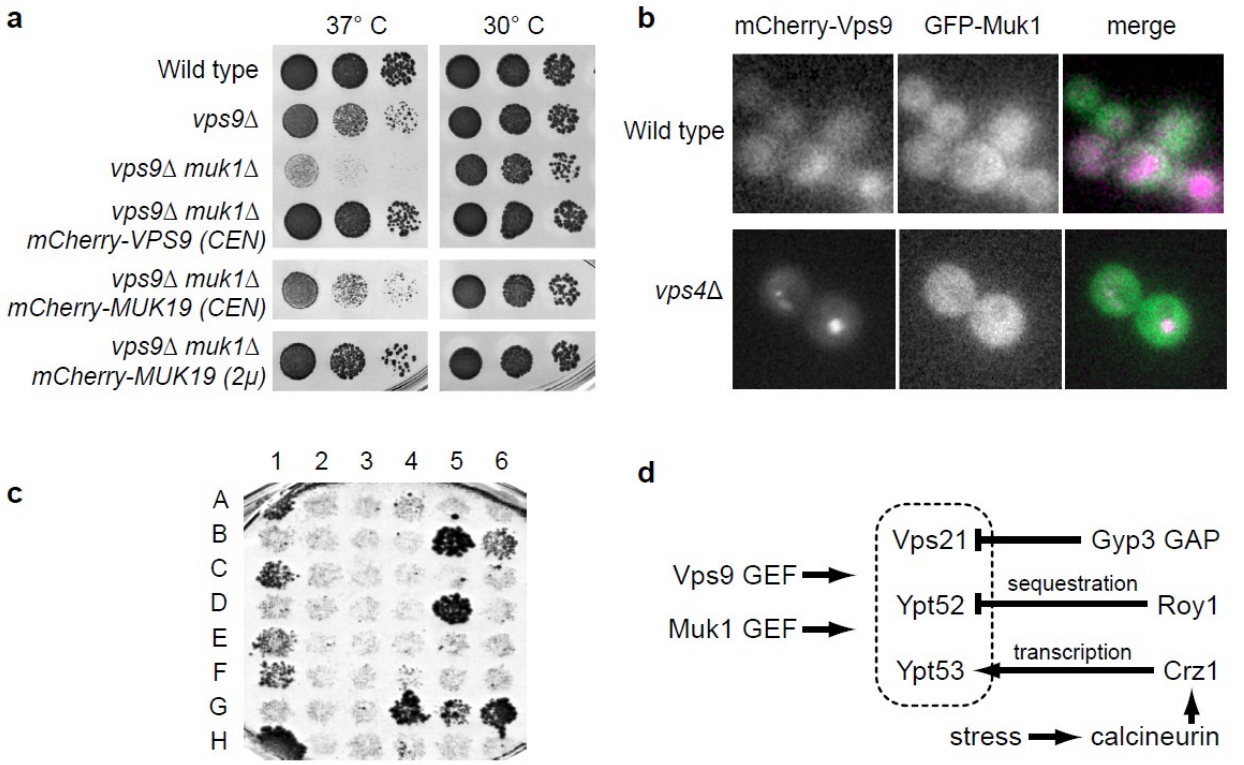

Figure 0-7 Muk1 and Vps9 localization, Muk1 interactions, and summary of Rab5 regulation in yeast. (A) Chimeric Muk1 and Vps9 constructs rescue heat sensitivity phenotypes of muk1Δ vps9Δ cells. Limiting dilution growth assay on YPD agar plates at 30°C and 37°C. Plasmid-borne chimeras were expressed using low copy (CEN) or high copy (2μ) plasmids. (B) GFP-Muk1 (green) and mCherry-Vps9 (purple) were coexpressed using low copy plasmids in the indicated strains and imaged. Both GFP-Muk1 and mCherry-Vps9 appear cytosolic in wild-type cells. GFP-Muk1 remains cytosolic in vps4Δ while mCherry-Vps9 accumulates at Class E compartments. (C) Yeast two hybrid (Y2H) interactions of Muk1. Muk1 was screened against potential interactors using a mating procedure as described in the Methods. The Y2H Plates were scored for growth on 3 mM 3-AT after 5 d at 30º C. The interactors and plate coordinates are summarized in Table 3. (D) Working model for regulation of signaling by the yeast Rab5 paralogs. See Discussion for details.

Discussion

VPS9 has been identified in several independent protein sorting screens, but MUK1 was not identified in any of these screens [6; 7; 9]. While high-throughput protein interaction screens and our yeast two-hybrid experiments suggest physical interactions between Muk1 and several other trafficking proteins [101; 102], Muk1's role in the endocytic network has not been examined until very recently. Deletion of Vps9 causes endolysosomal protein sorting and morphology defects [14]. These phenotypes were much less severe than combined deletion of the three Rab5 paralogs on which Vps9 acts, suggesting the presence of an additional Rab5 GEF. A combination of protein trafficking assays and *in vitro* biochemistry show that Muk1 is the second Rab5 GEF. While the present report was in preparation, Cabrera et al. reported parallel experiments independently showing that Muk1 has a Rab5 GEF activity [103].

Only one phenotypic defect arising from Muk1 deletion has so far been detected, a small but reproducible increase in the level of Ste3 in LUCID experiments (Figure 0-5C). This may reflect increased endocytic recycling of Ste3 to the plasma membrane, inefficient Ste3 transport into the vacuole lumen through the MVB pathway, or both. The traffic of other cargo molecules (CPY, CPS, Sna3, and Mup1) was not detectably impaired in *muk1*Δ single mutants. In contrast, *muk1*Δ *vps9*Δ double mutants had synthetic growth and trafficking defects stronger than both single mutants, and growth phenotypes similar to those of double and triple Rab5 knockout cells. Cabrera et. al. also observed that *muk1*Δ mutants had no overt phenotypes while *vps9*Δ mutants displayed only modest or no phenotype but that cells lacking both Vps9 and Muk1 showed prominent drug sensitivity and failed to properly localize subunits of the endosomal tethering and fusion machinery. Together these results indicate functional redundancy of Muk1 with Vps9 and help explain why Muk1 has eluded identification in forward genetic screens [103]. Conversely, overexpression of Muk1 appeared to slightly increase CPY secretion in wild-type cells (Figure 0-2B), demonstrating that normal Golgi-endosome cycling of the CPY receptor Vps10 is perturbed by high levels of Muk1.

As suggested by the presence of a VPS9-domain, Muk1 has nucleotide exchange activity against the three endocytic Rab5 paralogs (Vps21, Ypt52, and Ypt53), but it is unable to catalyze GDP release with Ypt7, the vacuolar Rab. Cabrera et al. similarly reported that Muk1 functions as a Rab GEF against Vps21 and Ypt52 [103]. A minor point of divergence is our finding that Vps9 and Muk1 stimulate comparable levels of nucleotide exchange on Ypt53. We note that different biochemical assays were employed in these studies. We assayed multiple-turnover hydrolysis of unmodified GTP, while Cabrera et al. monitored ejection of a Rab-bound fluorescent GDP analog.

Vps9 and Muk1 are mainly cytosolic in wild-type cells. However, in *vps4*Δ cells Vps9 becomes trapped at Class E compartments while Muk1 does not, demonstrating that Muk1 and Vps9 have distinct localization determinants and underscoring the possible functional specialization of these GEFs (Figure 0-7A).

GEF localization is a critical determinant of Rab localization and activity [74]. Mammalian Rabex-5, a VPS9-type GEF, is targeted to membranes by its effector, Rabaptin-5, which in turn interacts with proteins at Golgi, early, and late endosomal membranes [104-108]. In contrast Rin1, which also has a VPS9-domain, specifically localizes to internalized EGF receptor, which may ensure priority transit for receptor down regulation [109]. Yeast Vps9 binds mono-ubiquitylated cargo, which is hypothesized to localize Vps9 within the yeast endosomal network [71]. It is becoming clear that the VPS9 GEF family share a conserved catalytic domain, but that localization of individual GEFs to Rab5-positive membranes occurs through distinct modes of spatial and temporal regulation. Further investigation into

these varied mechanisms of localization will clarify how diverse Rab5-dependent trafficking pathways are regulated both in yeast and higher eukaryotes [110].

In the GEF cascade model proposed by Novick and colleagues, GEF localization is the key contributor to sequential Rab activation during compartmental maturation [111]. In the simplest form of this model, activated Rab "A" recruits a downstream GEF for Rab "B" as the membrane matures. Since Vps9 and Muk1 have distinct localization determinants but similar substrate specificities, it will be important to elucidate the normal order and locations of action of these GEFs.

Several studies have shown that even in the relatively simple yeast system, Rab5 signaling is subject to intricate regulation (Figure 0-7B). The three yeast Rab5 isoforms share overlapping capacities to support endolysosomal biogenesis and cargo transport [55; 77; 85], differentially control effector recruitment [103], and differ in their intrinsic ability to mediate vesicle tethering [76]. Ypt52 is typically held in an inactive state by Roy1 (Repressor Of Ypt52) [85], and Ypt53 expression is induced upon cellular stress as part of the Crz1-calcineurin regulon [77]. Moreover, Vps21 signaling is spatially and temporally restricted GAP Gyp3/Msb3 [77; 103]. It will be important to understand how these interactions govern specific cellular processes including stress responses [3], organelle inheritance [110], and metabolic regulation [112].

Materials and Methods

Cloning & Strain Construction

Strains and plasmids are summarized in Table 1. Generation of DNA cassettes to knock out the MUK1 ORF was performed as described [113] and correct integration was confirmed by genomic PCR mapping. Yeast expression plasmids were generated by gap repair recombination of PCR products into linearized plasmid vectors. GST-tagged Muk1 was inserted into the shuttle vector pFB-HTB-N [81]. The resulting plasmid was sequenced and transformed into DH10Bac E. coli and bacmid DNA was then purified. Bacmid DNA was transfected into Sf9 cells to prepare nuclear polyhedrosis baculovirus stocks. Yeast two-hybrid (Y2H) vectors are as described [23] or were obtained from the Yeast Resource Center (http://depts.washington.edu/yeastrc/). Vectors were sequence-verified prior to use.

Yeast-two-hybrid, culture & media

Yeast growth in liquid cultures was monitored using a Bioscreen machine (Growth Curves USA). 150 □ L cultures of YPD with or without 200 mM CaCl2 at 30° C were monitored with periodic shaking. Cultures were

inoculated at OD600nm = 0.1 from overnight YPD cultures. Bioscreen growth curve data were analyzed using YODA software [83] and plotted using GraphPad Prism 4.0. For solid media growth assays using limiting dilutions, cells were grown overnight at 30° C in synthetic media supplemented with casamino acids in order to select for retention of the MUK1 overexpression plasmid prior to serial dilution and application of cells to non-selective YPD plates. For Y2H tests, liquid cultures of the bait and prey Y2H library strains were grown in selective media then mixed in a 96-well plate and pinned to YPD plates using a 48-pin manifold. The plates were incubated at 30° C overnight, then colonies were replica plated onto synthetic media lacking Trp and Leu to select for diploid cells. These plates were incubated at 30° C for 2 days, then tested for Y2H interactions by replica plating to yeast synthetic media lacking Trp, Leu, and His, and supplemented with 3 mM 3-amino-1,2,4-triazole (3-AT). After 5 days at 30° C the plates were imaged.

Protein Purification

Vps9 and Gyp1-46 were expressed in E. coli and purified as described [76]. GST-tagged Rab G-proteins (Vps21, Ypt52, Ypt53, and Ypt7) were purified as described previously [77]. GST-Muk1 was expressed in adherent BTI-TN-5B1-4 (Hi-5) cells [82]. Cells were lysed by sonication in HEPES Lysis Buffer (50 mM HEPES, 150 mM NaCl, 5 mM 2-mercaptoethanol, pH 7.4) with protease inhibitors. The clarified lysate was bound to glutathione sepharose resin for 4 h at 4° C. The resin was extensively washed and eluted with 20 mM glutathione in HEPES Lysis Buffer. Excess glutathione was removed by exchange into HEPES Lysis Buffer using a PD-10 column (GE Healthcare). GST-Muk1 was then concentrated by ultrafiltration and snap-frozen in liquid nitrogen.

Microscopy

Fluorescence microscopy was performed with an Olympus IX71 light microscope, an EMCCD (Andor Ixon) camera, Pl 60× NA 1.45 or 100× NA 1.3 objectives, and appropriate filter sets. Andor IQ v.6.0.3.62 (Andor Bioimaging, Nottingham, UK) software was used for data collection. Image/J v.1.45s (J. Rasband, U.S. National Institutes of Health http://rsb.info.nih.gov/ij/), Photoshop v9.0 (Adobe) and Canvas v9.0 (ACD) software were used for contrast and brightness adjustments and for figure layout. For imaging of Mup1-GFP, yeast cells were grown overnight in selective defined media lacking methionine (Met) at 30° C and diluted to OD600nm 0.2 the following morning. 1.5 mL of culture was harvested at mid-log phase (~0.5-0.7 OD600nm) by sedimenting at 3,000 × g for 3 min., and suspended in 50 □ L fresh media lacking Met but containing 50 μM FM 4-64 styryl dye (Invitrogen). Cells were incubated for 15 min. at room temperature, centrifuged for 5 min. at 3,000 × g, and suspended in 1 mL of fresh media. This suspension was divided in

two with 1 mM methionine added to one portion and all samples were incubated at 30° C for 1 h. Suspensions were then centrifuged at 3,000 × g, suspended in 50 μL fresh media with or without Met, and imaged as described above.

GEF Activity Assays

EnzCheck Phosphate Assay Kit (Invitrogen E-6646) was used to measure GEF activities described previously [76]. Briefly, 100 μL aqueous reactions (total) containing reaction buffer (20 mM HEPES·NaOH pH 7.5, 150 mM NaCl, 25 mM MgCl2, 0.375 mM MESG, 0.5 mM GTP, 0.5% (m/v) BSA, and 2 U/mL purine nucleoside phosphorylase) and the indicated Rab at 20 μM were loaded into the wells of a 96-well plate (Corning) and allowed to equilibrate for 10 min. 0.5 μM Gyp1-46 was added and equilibrated for an additional 10 min., followed by addition of 2 μM GEF. A_{360nm} was then measured over time at 25-28° C in a Perkin Elmer Victor3 plate reader.

Trafficking Assays

Quantification of CPY-secretion was performed using a colorimetric assay as described [86]. LUCID assays were performed using a dual luciferase assay system (Promega) as described previously [77]. Briefly, cells were grown overnight at 30° C in synthetic dropout media containing 2% dextrose and supplemented with casamino acids, then diluted and grown in same media until log phase. After a 20 min. cyclohexamide chase (50 μg/mL final), ~0.5 OD600nm × mL log phase cells were collected by low-speed centrifugation, resuspended in 500 μL lysis buffer and lysed by vortexing with a slurry of glass beads at RT for 15 min. 5 μL aliquots of lysate were analyzed in opaque 96-well plates using a Perkin Elmer Victor Light Model 1420 luminometer. FLuc fusions and RLuc were expressed from a single plasmid. Signal from each cargo-FLuc fusion was normalized versus signal from soluble RLuc expressed from the constitutive PGK1 promoter.

LUCID time-course monitoring of Mup1-FLuc down-regulation employed cells incubated as described for microscopy experiments [93]. Briefly, cells were grown overnight in synthetic media (2% glucose) lacking methionine to maximize Mup1 retention at the plasma membrane. Note that media for LUCID assays of Mup1 cannot include casamino acids. A cyclohexamide chase was initiated 15 min before harvest and luminometric analysis as described above. Cells were diluted to approx. OD600nm ~ 0.15 and shaken at 30° C in low-Met media for 3 h. 1 mL aliquots were then transferred at intervals to culture tubes containing Met at a final concentration of 1 mM. Statistical analyses were performed using GraphPad Prism 4.0.

Organization of the HOPS Class C Core

Introduction

Traffic through the late endolysosomal compartments is regulated by sequential signaling of Rab5 and Rab7 subfamilies. As compartments mature along this pathway, Rab5 is replaced by Rab7 which is regulated by controlling the active state of each Rab via the CORVET and HOPS protein complexes. Briefly mentioned in Chapter 1, HOPS and CORVET share a conserved Vps-C protein core comprised of Vps11, Vps16, Vps18, and Vps33. This tetrameric core interacts with two accessory proteins at the endosomal membrane (Vps8, Vps3) to create CORVET and an alternate two accessory proteins (Vps39, Vps41) at the vacuolar membrane to create HOPS (Figure 0-1). Hybrid complexes containing an accessory proteins from each complex have indicated that these complexes may interconvert as the membrane matures; however, these hybrid have not yet been observed *in vivo* [49].

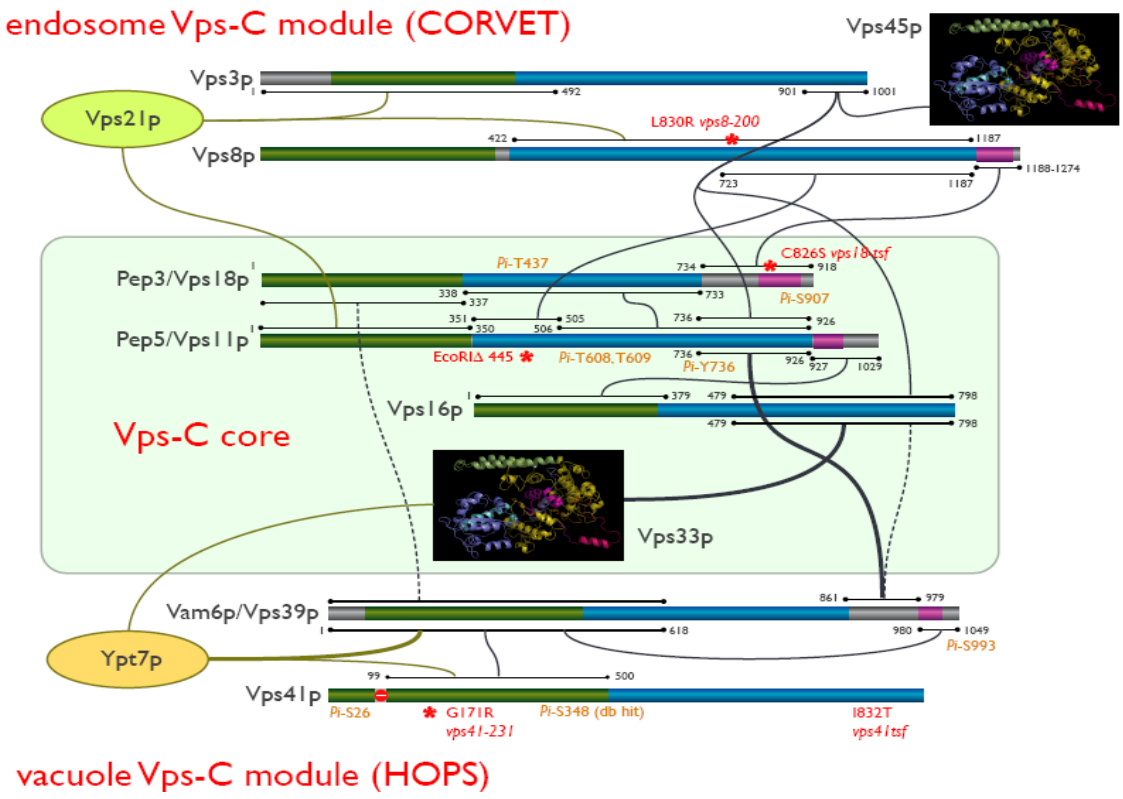

Figure 0-1 HOPS and CORVET Interaction Map

Previous domain mapping studies of these large hexameric complexes have indicated domains with homology to clathrin (Vps8, Vps11, Vps18, Vps39, Vps41), the COPI (**C**oat **P**rotein **C**omplex I) subunit (Vps39), WD40 motifs (Vps41) (Figure 0-2). Three of these proteins contain C-terminal RING motifs (Vps8, Vps11, Vps18) with a partial, or

pseudo, RING motif found in Vps39 which appears to lack residues to coordinate the second zinc ion. These RING domains are conserved from yeast to humans, with the Vps39 truncated RING domain absent but found instead on hsVps41. Examination of hsVps18 RING has shown it possesses non-specific E3 ligase activity toward crude E. coli lysate, though no studies have identified native substrates found at the vacuolar or endosomal surfaces [114].

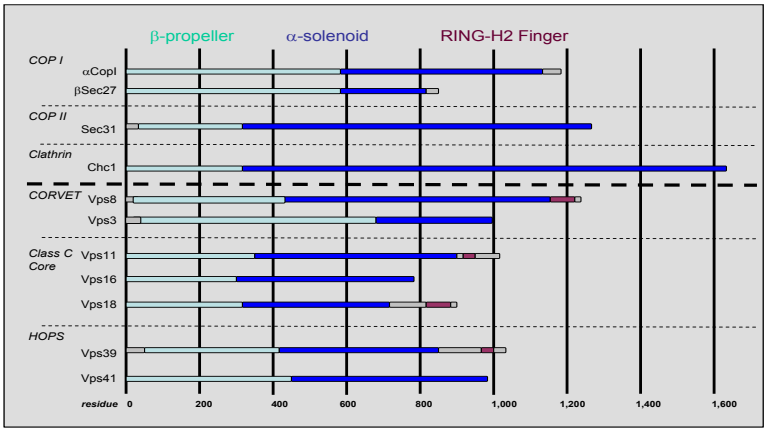


```
     C1 C2                                          C3H1  H2  C4                                        C5 C6
vps8  CEICGKKIWGAGLDPLLFLAWENVQRHQDMISVDLKTPLVIFKCHHGFHQTCLENLAQKPDEYS                                  CLICQ
vps11CFMCRLTLDIPVVFFK                                CGHIYHQHCLNEEEDTLESERKLFK                         CPKCLV
vps18CDECGKFLQIKKFIVFP                               CGHCFHWNCIIRVILNSNDYNLRQKTENFLKAKSKHNLNDLENIIVEKCGLCSD
vps39CPICKKVISNFGTDSISWFTREG                         RNIITHYNCGKVLQERFNAKNEKSSRIKQKTLGEVINELNNK
```

Figure 0-2 (A) Domain alignment of full protein (B) RING domain alignment.

Discussion

My work examining the RING motifs in the HOPS and CORVET complexes was part of a larger, collaborative study in the Merz lab. Published in 2011, it combined an extensive yeast-two-hybrid mapping of various HOPS and CORVET domains, *in vitro* biochemistry to assay trafficking pathways and binary protein-protein interactions, and *in vivo* microscopy studying vacuole and endosome morphology of various mutants. This work has been attached in Appendix-I, so I will simply summarize some of my contribution to this material.

The four RING domains were truncated and vacuole morphology was observed in cells expressing only mutant domain truncation mutants. With the exception of the Vps39 pseudo-RING, deletion of the RING domains result in vacuoles phenotypes which largely mimic their full gene counterparts (Figure 0-3A). Immediately upstream of the Vps39 pseudo-RING is a 120 residue unstructured region (Vps39 861-981) which also displayed a full deletion phenotype when removed. While RING domains are structural domains involved in protein-protein interactions, we believed that if these

were functioning as E3 ligases they may not be as essential in complex formation. This was clearly not the case, as deletion of the RING motifs resulted in either vacuole fragmentation (Vps11, Vps18, Vps39) or enlargement (Vps8) phenotypes. Yeast-two-hybrid results indicated that the Vps8 and Vps18 RING motifs may directly interact, which was also interesting since other RING domains heterodimers function as regulatory E3 ligases (i.e. BRCA1/BARD1, MDM2/MDMX). Vps11 appears to be a central structural component of the core, containing the most protein-protein interfaces as measured by yeast-two-hybrid. The Vps11 RING motif did not interact with any other RING domains, but instead with the N-terminal beta-propeller of Vps16. The Vps39 pseudo-RING had a weak interaction with its own N-terminus, possibly indicating some type of auto-inhibition. In order to examine this auto-inhibition theory I performed an *in vitro* vacuole fusion assay with recombinant Vps39 RING domain; however, no change in vacuole fusion was observed (Figure 0-3B).

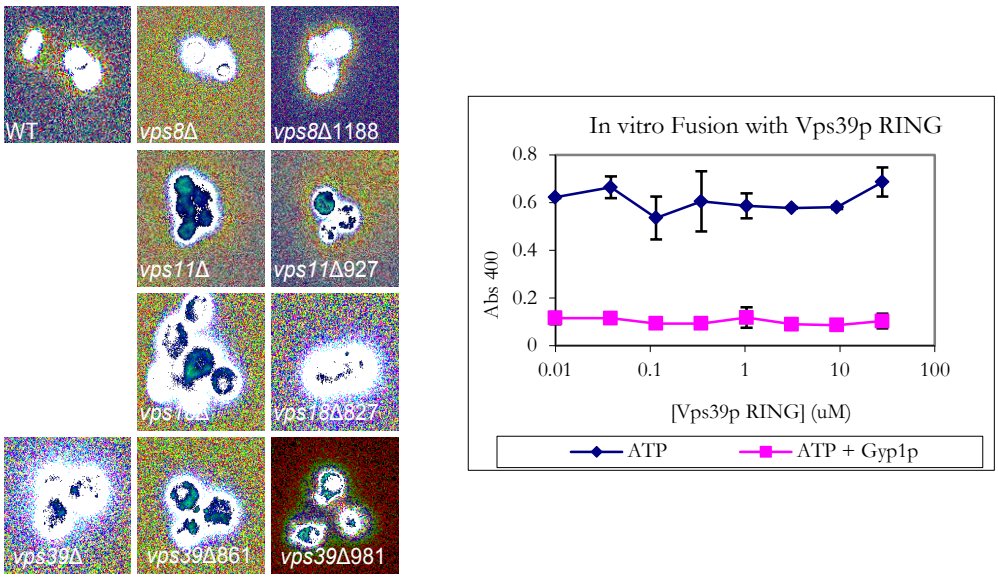

Figure 0-3 (A) Endosomal and vacuolar staining via FM4-64 in wild-type yeast and mutants with RING domain truncations. (B) *In vitro* vacuole fusion assay with recombinant Vps39 RING domain.

Discussion and Future Directions

Role of Ubiquitylation in Vps9 Localization and Activity

Vps9 binds ubiquitin via dimerization of its CUE domain, as revealed by its crystal structure and other *in vivo* and *in vitro* studies. Concurrently, Vps9 is modified with ubiquitin via the HECT E3 ubiquitin ligase Rsp5. This ubiquityl modification appears to account for only a small fraction of total cellular Vps9 (~10%) and its effects have remained unclear. Three models for how this modification may be affecting Vps9 activity or localization have been proposed. Ubiquitylation of Vps9 could (1) alter catalytic activity, (2) sequester the CUE domain, preventing interaction with ubiquitylated endocytic cargo and thus inhibiting localization to endosomes, or (3) allowing other unknown ubiquitin binding proteins to interact with Vps9 and target it to other cellular compartments.

I believe I have sufficiently shown that the first model, alteration of catalytic activity, is not occurring. The catalytic GEF activity of mono-ubiquitylated Vps9 does not appear to be significantly altered compared to non-ubiquitylated Vps9 as measured *in vitro*. I attempted to examine the *in vivo* role of CUE mutations on catalytic activation of Vps21 by creating an assay to quantify active Vps21. Unfortunately, this effort was largely unsuccessful.

A second hypothesis, the CUE-dependent localization of Vps9 to endocytic surfaces, is appealing for a number of reasons. It suggests that the high affinity CUE domain is responsible for helping Vps9 localize to endosomal surfaces where it can activate Vps21. This localization would be dependent on ubiquitylated cargo molecules on the endosomal limiting membranes and thus should enhance Vps21 activation at early endosomes which are rich in ubiquitylated cargo while impeding Vps9-dependent activation at later multivesicular bodies which contain little to no ubiquitin at their surface. Secondly, it reasons that the modification of Vps9 with ubiquitin could be intramolecular bound by the CUE domain, allowing for an alternate regulatory mode for Vps9. However, as appealing as this theory is, it has remained difficult to confirm.

As shown in Chapter 2, Vps9 is largely cytosolic which has made study of its subcellular localization difficult via microscopy or traditional subcellular fractionation experiments. Also, any modification which abolishes ubiquitin binding also abolishes ubiquitin modification via Rsp5. I believe a reconstituted liposome binding assay would help to examine this localization theory. In brief, reconstituted liposomes would be coated with Vps21 and ubiquitin or ubiquitylated cargo molecules, and then incubated with Vps9 or Vps9-Ub to examine their localization via floatation assays as well as their catalytic activity using a coupled enzymatic phosphate release assay. These reconstituted liposomes system would be a simple representation of ubiquitin decorated endosomes.

Three components are needed for this system to work: (1) binding of Vps21 to liposomes, (2) ubiquitin binding to liposomes, and (3) generation of ubiquitin-Vps9. Margaret Lo's work in the Merz Lab has shown that Vps21-His_{10} can be localized to liposomes bearing a small percentage of nickel-labeled lipids (1,2-di-(9Z-octadecenoyl)-*sN*-glycero-3-[(N-(5-amino-1-carboxypentyl)iminodiacetic acid)succinyl] "DOGS-NTA"). She then demonstrated that Vps21 on these liposomes can be activated with Vps9 and deactivated with Gyp1, a Vps21 GAP. With this first hurdle in hand, we simply need a method to conjugate ubiquitin to these liposomes. If we were to incorporate biotinylated lipids, along with the necessary DOGS-NTA for Vps21-His_{10} binding, a ubiquitin-avidin fusion protein could be localized to the membrane, creating a crude 'early endosomal' surface. As I have shown in Chapter 2, generation of ubiquitin-Vps9 is achievable.

It should then be possible to assay these reconstituted 'early endosomes' with recombinant Vps9 or Vps9-Ub. For example, liposome flotation assays would help determine if recombinant mono-ubiquitylated Vps9 is able to localize to the liposomes or if the ubiquityl moiety might prevent this. Reversible studies could also be performed where Usp2cc is spiked into the reaction in order to de-ubiquitylate Vps9. Modification of the C-terminal di-glycine residues on the ubiquitin-avidin protein should prevent Usp2cc from recognizing membrane bound ubiquitin.

In vitro phosphate release assays could examine reaction kinetics in this system and CUE domain mutations would be able to be examined more directly, helping to probe the theory that the CUE domain is essential in localizing Vps9 to early endosomes. I believe it would also be beneficial to begin structural studies of mono-ubiquitylated Vps9 in order to examine if the CUE domain is, as has been proposed, able to form an intramolecular interaction with the ubiquityl moiety.

Further Characterization of Muk1

As a result of my investigation into Vps9 activity and localization, I discovered Muk1 as a second VPS9 GEF in yeast. This protein did not appear in any of the several original VPS sorting screens or any subsequent high-throughput traffic screens. The phenotypes for deletion of Vps9 have always been relatively mild compared to deletion of the three Rab5 paralogs (Vps21, Ypt52, and Ypt53) and the deletion of Muk1 has no apparent phenotypes, however, deletion of both GEFs leads to severe defects. This indicates that each Rab5 GEF is able to compensate for the loss of the other. While beneficial from a cellular perspective, it has made characterization of Vps9 difficult. Subsequent studies of Vps9 localization and activity will have to be performed in Muk1 null yeast to examine Rab5 activation with CUE domain mutations.

Furthermore, the localization determinants of Muk1 need to be examined more closely. As more VPS9-domain containing proteins are discovered, it is becoming clear that regulation of their localization is a key method for regulating Rab5 activation. While Muk1 contains a central VPS9-domain, the remainder of the protein shows no homology toward previously identified protein domains. Due to the extensive Y2H studies in the Merz lab it should be straightforward to assay various domains of Muk1 against a library of endocytic proteins to examine possible interaction partners.

Vps10 is one of the best characterized recycling proteins which participate in retrograde traffic from endosomes to the late Golgi. Muk1 has been reported to interact with retromer subunits as well as the Golgi G-protein Ypt6. Our current studies of endocytic trafficking have shown few defects resulting in loss of Muk1. I believe that further examination of retrograde trafficking proteins, such as Vps10, may prove beneficial in examining Muk1's role in cellular transport.

The characterization of the rest of Muk1 will hopefully lead to a more complete understanding of where it may be functioning in the cell. These studies could help inform us of other Rab5-dependent trafficking events in the cell, or may instead clarify if Muk1 is simply a redundant GEF.

RING Domains in HOPS and CORVET

The four conserved, C-terminal RING domains in HOPS and CORVET have interested to many labs, with one study confirming non-specific E3 ligase activity of human hsVps18 against E. coli lysate. However, the roles for these domains have remained elusive. Since these motifs are integrated as part of large, multimeric protein complexes which are essential for endocytic trafficking, it has been challenging to examine them in isolation. As part of a study to find conditional HOPS mutants, a temperature sensitive allele of Vps18 (Vps18 C826S) was discovered in a screen[115]. This mutant has been shown to possess normal vacuole and endocytic morphology at permissive temperatures (30º C), but shows a Class C vacuole fragmentation phenotype when moved to elevated temperature (37º C). Remarkably, this transition is reversible if cells are returned to permissive temperature. While this mutation has been extensively used to study vacuole fragmentation phenotypes, one aspect has not been widely reported. This phenotype is a result of a single cysteine to serine point mutation in the first coordinating cysteine residue of the RING domain. Examining the ubiquitylation profiles of cells with this mutation, either at permissive or non-permissive temperatures, may begin to shed light on the possible role of this motif as an E3 ligase. It could also prove interesting to make similar mutations in the three other RING domains to examine if similar phenotypes are observed.

References

1. Klionsky D.J. and Emr S.D. (1990) A new class of lysosomal/vacuolar protein sorting signals. *J Biol Chem.* **265**, pp. 5349-5352
2. Stevens T., Esmon B. and Schekman R. (1982) Early stages in the yeast secretory pathway are required for transport of carboxypeptidase y to the vacuole. *Cell.* **30**, pp. 439-448
3. Marcusson E.G., Horazdovsky B.F., Cereghino J.L., Gharakhanian E. and Emr S.D. (1994) The sorting receptor for yeast vacuolar carboxypeptidase y is encoded by the vps10 gene. *Cell.* **77**, pp. 579-586
4. Deloche O., Yeung B.G., Payne G.S. and Schekman R. (2001) Vps10p transport from the trans-golgi network to the endosome is mediated by clathrin-coated vesicles. *Mol Biol Cell.* **12**, pp. 475-485
5. Deloche O. and Schekman R.W. (2002) Vps10p cycles between the tgn and the late endosome via the plasma membrane in clathrin mutants. *Mol Biol Cell.* **13**, pp. 4296-4307
6. Jones E.W. (1977) Proteinase mutants of saccharomyces cerevisiae. *Genetics.* **85**, pp. 23-33
7. Bankaitis V.A., Johnson L.M. and Emr S.D. (1986) Isolation of yeast mutants defective in protein targeting to the vacuole. *Proc Natl Acad Sci U S A.* **83**, pp. 9075-9079
8. Rothman J.H. and Stevens T.H. (1986) Protein sorting in yeast: mutants defective in vacuole biogenesis mislocalize vacuolar proteins into the late secretory pathway. *Cell.* **47**, pp. 1041-1051
9. Raymond C.K., Howald-Stevenson I., Vater C.A. and Stevens T.H. (1992) Morphological classification of the yeast vacuolar protein sorting mutants: evidence for a prevacuolar compartment in class e vps mutants. *Mol Biol Cell.* **3**, pp. 1389-1402
10. Babst M., Katzmann D.J., Estepa-Sabal E.J., Meerloo T. and Emr S.D. (2002) Escrt-iii: an endosome-associated heterooligomeric protein complex required for mvb sorting. *Dev Cell.* **3**, pp. 271-282
11. Babst M., Katzmann D.J., Snyder W.B., Wendland B. and Emr S.D. (2002) Endosome-associated complex, escrt-ii, recruits transport machinery for protein sorting at the multivesicular body. *Dev Cell.* **3**, pp. 283-289
12. Katzmann D.J., Stefan C.J., Babst M. and Emr S.D. (2003) Vps27 recruits escrt machinery to endosomes during mvb sorting. *J Cell Biol.* **162**, pp. 413-423
13. Azmi I.F., Davies B.A., Xiao J., Babst M., Xu Z. and Katzmann D.J. (2008) Escrt-iii family members stimulate vps4 atpase activity directly or via vta1. *Dev Cell.* **14**, pp. 50-61
14. Burd C.G., Mustol P.A., Schu P.V. and Emr S.D. (1996) A yeast protein related to a mammalian ras-binding protein, vps9p, is required for localization of vacuolar proteins. *Mol Cell Biol.* **16**, pp. 2369-2377
15. Hama H., Tall G.G. and Horazdovsky B.F. (1999) Vps9p is a guanine nucleotide exchange factor involved in vesicle-mediated vacuolar protein transport. *J Biol Chem.* **274**, pp. 15284-15291
16. Nottingham R.M. and Pfeffer S.R. (2009) Defining the boundaries: rab gefs and gaps. *Proc Natl Acad Sci U S A.* **106**, pp. 14185-14186
17. Peterson M.R., Burd C.G. and Emr S.D. (1999) Vac1p coordinates rab and phosphatidylinositol 3-kinase signaling in vps45p-dependent vesicle docking/fusion at the endosome. *Curr Biol.* **9**, pp. 159-162
18. Tall G.G., Hama H., DeWald D.B. and Horazdovsky B.F. (1999) The phosphatidylinositol 3-phosphate binding protein vac1p interacts with a rab gtpase and a sec1p homologue to facilitate vesicle-mediated vacuolar protein sorting. *Mol Biol Cell.* **10**, pp. 1873-1889
19. Cowles C.R., Emr S.D. and Horazdovsky B.F. (1994) Mutations in the vps45 gene, a sec1 homologue, result in vacuolar protein sorting defects and accumulation of membrane vesicles. *J Cell Sci.* **107 (Pt 12)**, pp. 3449-3459
20. Piper R.C., Whitters E.A. and Stevens T.H. (1994) Yeast vps45p is a sec1p-like protein required for the consumption of vacuole-targeted, post-golgi transport vesicles. *Eur J Cell Biol.* **65**, pp. 305-318
21. Scales S.J., Chen Y.A., Yoo B.Y., Patel S.M., Doung Y.C. and Scheller R.H. (2000) Snares contribute to the specificity of membrane fusion. *Neuron.* **26**, pp. 457-464
22. Seaman M.N., Marcusson E.G., Cereghino J.L. and Emr S.D. (1997) Endosome to golgi retrieval of the vacuolar protein sorting receptor, vps10p, requires the function of the vps29, vps30, and vps35 gene products. *J Cell Biol.* **137**, pp. 79-92
23. Burda P., Padilla S.M., Sarkar S. and Emr S.D. (2002) Retromer function in endosome-to-golgi retrograde transport is regulated by the yeast vps34 ptdins 3-kinase. *J Cell Sci.* **115**, pp. 3889-3900
24. Seaman M.N.J. and Williams H.P. (2002) Identification of the functional domains of yeast sorting nexins vps5p and vps17p. *Mol Biol Cell.* **13**, pp. 2826-2840
25. McGough I.J. and Cullen P.J. (2013) Clathrin is not required for snx-bar-retromer-mediated carrier formation. *J Cell Sci.* **126**, pp. 45-52

26. Siniossoglou S. and Pelham H.R. (2001) An effector of ypt6p binds the snare tlg1p and mediates selective fusion of vesicles with late golgi membranes. *EMBO J*. **20**, pp. 5991-5998
27. Conibear E., Cleck J.N. and Stevens T.H. (2003) Vps51p mediates the association of the garp (vps52/53/54) complex with the late golgi t-snare tlg1p. *Mol Biol Cell*. **14**, pp. 1610-1623
28. Reggiori F., Wang C., Stromhaug P.E., Shintani T. and Klionsky D.J. (2003) Vps51 is part of the yeast vps fifty-three tethering complex essential for retrograde traffic from the early endosome and cvt vesicle completion. *J Biol Chem*. **278**, pp. 5009-5020
29. Hicke L. (2001) Protein regulation by monoubiquitin. *Nat Rev Mol Cell Biol*. **2**, pp. 195-201
30. Odorizzi G., Katzmann D.J., Babst M., Audhya A. and Emr S.D. (2003) Bro1 is an endosome-associated protein that functions in the mvb pathway in saccharomyces cerevisiae. *J Cell Sci*. **116**, pp. 1893-1903
31. Davis N.G., Horecka J.L. and Sprague G.F.J. (1993) Cis- and trans-acting functions required for endocytosis of the yeast pheromone receptors. *J Cell Biol*. **122**, pp. 53-65
32. Roth A.F. and Davis N.G. (1996) Ubiquitination of the yeast a-factor receptor. *J Cell Biol*. **134**, pp. 661-674
33. Macdonald C., Stringer D.K. and Piper R.C. (2012) Sna3 is an rsp5 adaptor protein that relies on ubiquitination for its mvb sorting. *Traffic*. **13**, pp. 586-598
34. Rotin D., Staub O. and Haguenauer-Tsapis R. (2000) Ubiquitination and endocytosis of plasma membrane proteins: role of nedd4/rsp5p family of ubiquitin-protein ligases. *J Membr Biol*. **176**, pp. 1-17
35. Wendland B. (2002) Epsins: adaptors in endocytosis?. *Nat Rev Mol Cell Biol*. **3**, pp. 971-977
36. Hershko A., Heller H., Elias S. and Ciechanover A. (1983) Components of ubiquitin-protein ligase system. resolution, affinity purification, and role in protein breakdown. *J Biol Chem*. **258**, pp. 8206-8214
37. Joazeiro C.A. and Weissman A.M. (2000) Ring finger proteins: mediators of ubiquitin ligase activity. *Cell*. **102**, pp. 549-552
38. Hurley J.H., Lee S. and Prag G. (2006) Ubiquitin-binding domains. *Biochem J*. **399**, pp. 361-372
39. Hofmann K. and Falquet L. (2001) A ubiquitin-interacting motif conserved in components of the proteasomal and lysosomal protein degradation systems. *Trends Biochem Sci*. **26**, pp. 347-350
40. Hofmann K. and Bucher P. (1995) The rsp5-domain is shared by proteins of diverse functions. *FEBS Lett*. **358**, pp. 153-157
41. Ponting C.P. (2000) Proteins of the endoplasmic-reticulum-associated degradation pathway: domain detection and function prediction. *Biochem J*. **351 Pt 2**, pp. 527-535
42. Katzmann D.J., Babst M. and Emr S.D. (2001) Ubiquitin-dependent sorting into the multivesicular body pathway requires the function of a conserved endosomal protein sorting complex, escrt-i. *Cell*. **106**, pp. 145-155
43. Bilodeau P.S., Urbanowski J.L., Winistorfer S.C. and Piper R.C. (2002) The vps27p hse1p complex binds ubiquitin and mediates endosomal protein sorting. *Nat Cell Biol*. **4**, pp. 534-539
44. Shih S.C., Katzmann D.J., Schnell J.D., Sutanto M., Emr S.D. and Hicke L. (2002) Epsins and vps27p/hrs contain ubiquitin-binding domains that function in receptor endocytosis. *Nat Cell Biol*. **4**, pp. 389-393
45. Babst M., Sato T.K., Banta L.M. and Emr S.D. (1997) Endosomal transport function in yeast requires a novel aaa-type atpase, vps4p. *EMBO J*. **16**, pp. 1820-1831
46. Babst M., Wendland B., Estepa E.J. and Emr S.D. (1998) The vps4p aaa atpase regulates membrane association of a vps protein complex required for normal endosome function. *EMBO J*. **17**, pp. 2982-2993
47. Grosshans B.L., Ortiz D. and Novick P. (2006) Rabs and their effectors: achieving specificity in membrane traffic. *Proc Natl Acad Sci U S A*. **103**, pp. 11821-11827
48. Wichmann H., Hengst L. and Gallwitz D. (1992) Endocytosis in yeast: evidence for the involvement of a small gtp-binding protein (ypt7p). *Cell*. **71**, pp. 1131-1142
49. Peplowska K., Markgraf D.F., Ostrowicz C.W., Bange G. and Ungermann C. (2007) The corvet tethering complex interacts with the yeast rab5 homolog vps21 and is involved in endo-lysosomal biogenesis. *Dev Cell*. **12**, pp. 739-750
50. Bock J.B., Matern H.T., Peden A.A. and Scheller R.H. (2001) A genomic perspective on membrane compartment organization. *Nature*. **409**, pp. 839-841
51. Gorvel J.P., Chavrier P., Zerial M. and Gruenberg J. (1991) Rab5 controls early endosome fusion in vitro. *Cell*. **64**, pp. 915-925
52. Bucci C., Parton R.G., Mather I.H., Stunnenberg H., Simons K., Hoflack B. and Zerial M. (1992) The small gtpase rab5 functions as a regulatory factor in the early endocytic pathway. *Cell*. **70**, pp. 715-728
53. Nielsen E., Severin F., Backer J.M., Hyman A.A. and Zerial M. (1999) Rab5 regulates motility of early endosomes on microtubules. *Nat Cell Biol*. **1**, pp. 376-382
54. Bucci C., Lütcke A., Steele-Mortimer O., Olkkonen V.M., Dupree P., Chiariello M., Bruni C.B., Simons K. and Zerial M. (1995) Co-operative regulation of endocytosis by three rab5 isoforms. *FEBS Lett*. **366**, pp. 65-71

55. Singer-Krüger B., Stenmark H., Düsterhöft A., Philippsen P., Yoo J.S., Gallwitz D. and Zerial M. (1994) Role of three rab5-like gtpases, ypt51p, ypt52p, and ypt53p, in the endocytic and vacuolar protein sorting pathways of yeast. *J Cell Biol.* **125**, pp. 283-298
56. Horazdovsky B.F., Busch G.R. and Emr S.D. (1994) Vps21 encodes a rab5-like gtp binding protein that is required for the sorting of yeast vacuolar proteins. *EMBO J.* **13**, pp. 1297-1309
57. Cherfils J. and Chardin P. (1999) Gefs: structural basis for their activation of small gtp-binding proteins. *Trends Biochem Sci.* **24**, pp. 306-311
58. Yoshimura S., Gerondopoulos A., Linford A., Rigden D.J. and Barr F.A. (2010) Family-wide characterization of the denn domain rab gdp-gtp exchange factors. *J Cell Biol.* **191**, pp. 367-381
59. Horiuchi H., Lippé R., McBride H.M., Rubino M., Woodman P., Stenmark H., Rybin V., Wilm M., Ashman K., Mann M. and Zerial M. (1997) A novel rab5 gdp/gtp exchange factor complexed to rabaptin-5 links nucleotide exchange to effector recruitment and function. *Cell.* **90**, pp. 1149-1159
60. Tall G.G., Barbieri M.A., Stahl P.D. and Horazdovsky B.F. (2001) Ras-activated endocytosis is mediated by the rab5 guanine nucleotide exchange activity of rin1. *Dev Cell.* **1**, pp. 73-82
61. Kajiho H., Saito K., Tsujita K., Kontani K., Araki Y., Kurosu H. and Katada T. (2003) Rin3: a novel rab5 gef interacting with amphiphysin ii involved in the early endocytic pathway. *J Cell Sci.* **116**, pp. 4159-4168
62. Saito K., Murai J., Kajiho H., Kontani K., Kurosu H. and Katada T. (2002) A novel binding protein composed of homophilic tetramer exhibits unique properties for the small gtpase rab5. *J Biol Chem.* **277**, pp. 3412-3418
63. Esters H., Alexandrov K., Iakovenko A., Ivanova T., Thomä N., Rybin V., Zerial M., Scheidig A.J. and Goody R.S. (2001) Vps9, rabex-5 and dss4: proteins with weak but distinct nucleotide-exchange activities for rab proteins. *J Mol Biol.* **310**, pp. 141-156
64. Lee S., Tsai Y.C., Mattera R., Smith W.J., Kostelansky M.S., Weissman A.M., Bonifacino J.S. and Hurley J.H. (2006) Structural basis for ubiquitin recognition and autoubiquitination by rabex-5. *Nat Struct Mol Biol.* **13**, pp. 264-271
65. Penengo L., Mapelli M., Murachelli A.G., Confalonieri S., Magri L., Musacchio A., Di Fiore P.P., Polo S. and Schneider T.R. (2006) Crystal structure of the ubiquitin binding domains of rabex-5 reveals two modes of interaction with ubiquitin. *Cell.* **124**, pp. 1183-1195
66. Kang R.S., Daniels C.M., Francis S.A., Shih S.C., Salerno W.J., Hicke L. and Radhakrishnan I. (2003) Solution structure of a cue-ubiquitin complex reveals a conserved mode of ubiquitin binding. *Cell.* **113**, pp. 621-630
67. Prag G., Misra S., Jones E.A., Ghirlando R., Davies B.A., Horazdovsky B.F. and Hurley J.H. (2003) Mechanism of ubiquitin recognition by the cue domain of vps9p. *Cell.* **113**, pp. 609-620
68. Shih S.C., Prag G., Francis S.A., Sutanto M.A., Hurley J.H. and Hicke L. (2003) A ubiquitin-binding motif required for intramolecular monoubiquitylation, the cue domain. *EMBO J.* **22**, pp. 1273-1281
69. Haglund K., Di Fiore P.P. and Dikic I. (2003) Distinct monoubiquitin signals in receptor endocytosis. *Trends Biochem Sci.* **28**, pp. 598-603
70. Hicke L. and Dunn R. (2003) Regulation of membrane protein transport by ubiquitin and ubiquitin-binding proteins. *Annu Rev Cell Dev Biol.* **19**, pp. 141-172
71. Davies B.A., Topp J.D., Sfeir A.J., Katzmann D.J., Carney D.S., Tall G.G., Friedberg A.S., Deng L., Chen Z. and Horazdovsky B.F. (2003) Vps9p cue domain ubiquitin binding is required for efficient endocytic protein traffic. *J Biol Chem.* **278**, pp. 19826-19833
72. Donaldson K.M., Yin H., Gekakis N., Supek F. and Joazeiro C.A.P. (2003) Ubiquitin signals protein trafficking via interaction with a novel ubiquitin binding domain in the membrane fusion regulator, vps9p. *Curr Biol.* **13**, pp. 258-262
73. Carney D.S., Davies B.A. and Horazdovsky B.F. (2006) Vps9 domain-containing proteins: activators of rab5 gtpases from yeast to neurons. *Trends Cell Biol.* **16**, pp. 27-35
74. Blümer J., Rey J., Dehmelt L., Mazel T., Wu Y., Bastiaens P., Goody R.S. and Itzen A. (2013) Rabgefs are a major determinant for specific rab membrane targeting. *J Cell Biol.* **200**, pp. 287-300
75. Singer-Krüger B., Stenmark H. and Zerial M. (1995) Yeast ypt51p and mammalian rab5: counterparts with similar function in the early endocytic pathway. *J Cell Sci.* **108 (Pt 11)**, pp. 3509-3521
76. Lo S., Brett C.L., Plemel R.L., Vignali M., Fields S., Gonen T. and Merz A.J. (2012) Intrinsic tethering activity of endosomal rab proteins. *Nat Struct Mol Biol.* **19**, pp. 40-47
77. Nickerson D.P., Russell M.R.G., Lo S., Chapin H.C., Milnes J.M. and Merz A.J. (2012) Termination of isoform-selective vps21/rab5 signaling at endolysosomal organelles by msb3/gyp3. *Traffic.* **13**, pp. 1411-1428
78. Abdul-Ghani M., Gougeon P.Y., Prosser D.C., Da-Silva L.F. and Ngsee J.K. (2001) Pra isoforms are targeted to distinct membrane compartments. *J Biol Chem.* **276**, pp. 6225-6233
79. Collins R.N. (2003) "getting it on"--gdi displacement and small gtpase membrane recruitment. *Mol Cell.* **12**, pp. 1064-1066
80. Sivars U., Aivazian D. and Pfeffer S.R. (2003) Yip3 catalyses the dissociation of endosomal rab-gdi complexes. *Nature.* **425**, pp. 856-859

81. Brett C.L., Plemel R.L., Lobingier B.T., Vignali M., Fields S. and Merz A.J. (2008) Efficient termination of vacuolar rab gtpase signaling requires coordinated action by a gap and a protein kinase. *J Cell Biol.* **182**, pp. 1141-1151
82. Plemel R.L., Lobingier B.T., Brett C.L., Angers C.G., Nickerson D.P., Paulsel A., Sprague D. and Merz A.J. (2011) Subunit organization and rab interactions of vps-c protein complexes that control endolysosomal membrane traffic. *Mol Biol Cell.* **22**, pp. 1353-1363
83. Olsen B., Murakami C.J. and Kaeberlein M. (2010) Yoda: software to facilitate high-throughput analysis of chronological life span, growth rate, and survival in budding yeast. *BMC Bioinformatics.* **11**, p. 141
84. Samanta M.P. and Liang S. (2003) Predicting protein functions from redundancies in large-scale protein interaction networks. *Proc Natl Acad Sci U S A.* **100**, pp. 12579-12583
85. Liu Y., Nakatsukasa K., Kotera M., Kanada A., Nishimura T., Kishi T., Mimura S. and Kamura T. (2011) Non-scf-type f-box protein roy1/ymr258c interacts with a rab5-like gtpase ypt52 and inhibits ypt52 function. *Mol Biol Cell.* **22**, pp. 1575-1584
86. Darsow T., Odorizzi G. and Emr S.D. (2000) Invertase fusion proteins for analysis of protein trafficking in yeast. *Methods Enzymol.* **327**, pp. 95-106
87. McNatt M.W., McKittrick I., West M. and Odorizzi G. (2007) Direct binding to rsp5 mediates ubiquitin-independent sorting of sna3 via the multivesicular body pathway. *Mol Biol Cell.* **18**, pp. 697-706
88. Stawiecka-Mirota M., Pokrzywa W., Morvan J., Zoladek T., Haguenauer-Tsapis R., Urban-Grimal D. and Morsomme P. (2007) Targeting of sna3p to the endosomal pathway depends on its interaction with rsp5p and multivesicular body sorting on its ubiquitylation. *Traffic.* **8**, pp. 1280-1296
89. Oestreich A.J., Aboian M., Lee J., Azmi I., Payne J., Issaka R., Davies B.A. and Katzmann D.J. (2007) Characterization of multiple multivesicular body sorting determinants within sna3: a role for the ubiquitin ligase rsp5. *Mol Biol Cell.* **18**, pp. 707-720
90. Chen L. and Davis N.G. (2000) Recycling of the yeast a-factor receptor. *J Cell Biol.* **151**, pp. 731-738
91. Albert S. and Gallwitz D. (2000) Msb4p, a protein involved in cdc42p-dependent organization of the actin cytoskeleton, is a ypt/rab-specific gap. *Biol Chem.* **381**, pp. 453-456
92. Tsukada M. and Gallwitz D. (1996) Isolation and characterization of sys genes from yeast, multicopy suppressors of the functional loss of the transport gtpase ypt6p. *J Cell Sci.* **109 (Pt 10)**, pp. 2471-2481
93. Menant A., Barbey R. and Thomas D. (2006) Substrate-mediated remodeling of methionine transport by multiple ubiquitin-dependent mechanisms in yeast cells. *EMBO J.* **25**, pp. 4436-4447
94. MacDonald C., Buchkovich N.J., Stringer D.K., Emr S.D. and Piper R.C. (2012) Cargo ubiquitination is essential for multivesicular body intralumenal vesicle formation. *EMBO Rep.* **13**, pp. 331-338
95. Odorizzi G., Babst M. and Emr S.D. (1998) Fab1p ptdins(3)p 5-kinase function essential for protein sorting in the multivesicular body. *Cell.* **95**, pp. 847-858
96. Nickerson D.P., West M. and Odorizzi G. (2006) Did2 coordinates vps4-mediated dissociation of escrt-iii from endosomes. *J Cell Biol.* **175**, pp. 715-720
97. Pan X., Eathiraj S., Munson M. and Lambright D.G. (2006) Tbc-domain gaps for rab gtpases accelerate gtp hydrolysis by a dual-finger mechanism. *Nature.* **442**, pp. 303-306
98. Webb M.R. (1992) A continuous spectrophotometric assay for inorganic phosphate and for measuring phosphate release kinetics in biological systems. *Proc Natl Acad Sci U S A.* **89**, pp. 4884-4887
99. Russell M.R.G., Shideler T., Nickerson D.P., West M. and Odorizzi G. (2012) Class e compartments form in response to escrt dysfunction in yeast due to hyperactivity of the vps21 rab gtpase. *J Cell Sci.* **125**, pp. 5208-5220
100. Costanzo M., Baryshnikova A., Bellay J., Kim Y., Spear E.D., Sevier C.S., Ding H., Koh J.L.Y., Toufighi K., Mostafavi S., Prinz J., St Onge R.P., VanderSluis B., Makhnevych T., Vizeacoumar F.J., Alizadeh S., Bahr S., Brost R.L., Chen Y., Cokol M., Deshpande R., Li Z., Lin Z., Liang W., Marback M., Paw J., San Luis B., Shuteriqi E., Tong A.H.Y., van Dyk N., Wallace I.M., Whitney J.A., Weirauch M.T., Zhong G., Zhu H., Houry W.A., Brudno M., Ragibizadeh S., Papp B., Pál C., Roth F.P., Giaever G., Nislow C., Troyanskaya O.G., Bussey H., Bader G.D., Gingras A., Morris Q.D., Kim P.M., Kaiser C.A., Myers C.L., Andrews B.J. and Boone C. (2010) The genetic landscape of a cell. *Science.* **327**, pp. 425-431
101. Uetz P. and Hughes R.E. (2000) Systematic and large-scale two-hybrid screens. *Curr Opin Microbiol.* **3**, pp. 303-308
102. Yu H., Braun P., Yildirim M.A., Lemmens I., Venkatesan K., Sahalie J., Hirozane-Kishikawa T., Gebreab F., Li N., Simonis N., Hao T., Rual J., Dricot A., Vazquez A., Murray R.R., Simon C., Tardivo L., Tam S., Svrzikapa N., Fan C., de Smet A., Motyl A., Hudson M.E., Park J., Xin X., Cusick M.E., Moore T., Boone C., Snyder M., Roth F.P., Barabási A., Tavernier J., Hill D.E. and Vidal M. (2008) High-quality binary protein interaction map of the yeast interactome network. *Science.* **322**, pp. 104-110
103. Cabrera M., Arlt H., Epp N., Lachmann J., Griffith J., Perz A., Reggiori F. and Ungermann C. (2013) Functional separation of endosomal fusion factors and the class c core vacuole/endosome tethering (corvet) complex in endosome biogenesis. *J Biol Chem.* **288**, pp. 5166-5175

104. McBride H.M., Rybin V., Murphy C., Giner A., Teasdale R. and Zerial M. (1999) Oligomeric complexes link rab5 effectors with nsf and drive membrane fusion via interactions between eea1 and syntaxin 13. *Cell***.** **98**, pp. 377-386
105. Hirst J., Lui W.W., Bright N.A., Totty N., Seaman M.N. and Robinson M.S. (2000) A family of proteins with gamma-adaptin and vhs domains that facilitate trafficking between the trans-golgi network and the vacuole/lysosome. *J Cell Biol***.** **149**, pp. 67-80
106. Zhu Y., Doray B., Poussu A., Lehto V.P. and Kornfeld S. (2001) Binding of gga2 to the lysosomal enzyme sorting motif of the mannose 6-phosphate receptor. *Science***.** **292**, pp. 1716-1718
107. Shiba Y., Takatsu H., Shin H. and Nakayama K. (2002) Gamma-adaptin interacts directly with rabaptin-5 through its ear domain. *J Biochem***.** **131**, pp. 327-336
108. Mattera R., Arighi C.N., Lodge R., Zerial M. and Bonifacino J.S. (2003) Divalent interaction of the ggas with the rabaptin-5-rabex-5 complex. *EMBO J***.** **22**, pp. 78-88
109. Barbieri M.A., Kong C., Chen P., Horazdovsky B.F. and Stahl P.D. (2003) The src homology 2 domain of rin1 mediates its binding to the epidermal growth factor receptor and regulates receptor endocytosis. *J Biol Chem***.** **278**, pp. 32027-32036
110. Weisman L.S. (2006) Organelles on the move: insights from yeast vacuole inheritance. *Nat Rev Mol Cell Biol***.** **7**, pp. 243-252
111. Mizuno-Yamasaki E., Medkova M., Coleman J. and Novick P. (2010) Phosphatidylinositol 4-phosphate controls both membrane recruitment and a regulatory switch of the rab gef sec2p. *Dev Cell***.** **18**, pp. 828-840
112. Bridges D., Fisher K., Zolov S.N., Xiong T., Inoki K., Weisman L.S. and Saltiel A.R. (2012) Rab5 proteins regulate activation and localization of target of rapamycin complex 1. *J Biol Chem***.** **287**, pp. 20913-20921
113. Gueldener U., Heinisch J., Koehler G.J., Voss D. and Hegemann J.H. (2002) A second set of loxp marker cassettes for cre-mediated multiple gene knockouts in budding yeast. *Nucleic Acids Res***.** **30**, p. e23
114. Yogosawa S., Hatakeyama S., Nakayama K.I., Miyoshi H., Kohsaka S. and Akazawa C. (2005) Ubiquitylation and degradation of serum-inducible kinase by hvps18, a ring-h2 type ubiquitin ligase. *J Biol Chem***.** **280**, pp. 41619-41627
115. Rieder S.E. and Emr S.D. (1997) A novel ring finger protein complex essential for a late step in protein transport to the yeast vacuole. *Mol Biol Cell***.** **8**, pp. 2307-2327

Appendix I